



Published in final edited form as:

Biochem Pharmacol. 2008 August 15; 76(4): 552–567. doi:10.1016/j.bcp.2008.05.016.

Role of Mitochondrial Dysfunction in Cellular Responses to *S*-(1,2-Dichlorovinyl)-L-cysteine in Primary Cultures of Human Proximal Tubular Cells

Feng Xu, Irene Papanayotou, David A. Putt, Jian Wang, and Lawrence H. Lash

Department of Pharmacology Wayne State University School of Medicine Detroit, MI 48201

Abstract

The nephrotoxic metabolite of the environmental contaminant trichloroethylene, *S*-(1,2-dichlorovinyl)-L-cysteine (DCVC), is known to elicit cytotoxicity in rat and human proximal tubular (rPT and hPT, respectively) cells that involves inhibition of mitochondrial function. DCVC produces a range of cytotoxic and compensatory responses in hPT cells, depending on dose and exposure time, including necrosis, apoptosis, repair, and enhanced cell proliferation. The present study tested the hypothesis that induction of mitochondrial dysfunction is an obligatory step in the cytotoxicity caused by DCVC in primary cultures of hPT cells. DCVC-induced necrosis was primarily a high-concentration ($\geq 50 \mu\text{M}$) and late ($\geq 24 \text{ hr}$) response whereas apoptosis and increased proliferation occurred at relatively low concentrations ($< 50 \mu\text{M}$) and early time points ($\leq 24 \text{ hr}$). Decreases in cellular DNA content, indicative of cell loss, were observed at DCVC concentrations as low as $1 \mu\text{M}$. Involvement of mitochondrial dysfunction in DCVC-induced cytotoxicity was supported by showing that DCVC caused modest depletion of cellular ATP, inhibition of respiration, and activation of caspase-3/7. Cyclosporin A protected cells against DCVC-induced apoptosis and both cyclosporin A and ruthenium red protected cells against DCVC-induced loss of mitochondrial membrane potential. DCVC caused little or no activation of caspase-8 and did not significantly induce expression of Fas receptor, consistent with apoptosis occurring only by the mitochondrial pathway. These results support the conclusion that mitochondrial dysfunction is an early and obligatory step in DCVC-induced cytotoxicity in hPT cells.

Keywords

mitochondrial energetics; human proximal tubular cells; apoptosis; cell proliferation; cytotoxicity; FasR; caspase activation

1. Introduction

Trichloroethylene (TRI; also known as trichloroethene and sometimes abbreviated as TCE) is an environmental contaminant that is considered a known animal carcinogen and a “probable human carcinogen” by the International Agency for Research on Cancer [1] and as “reasonably anticipated to be a human carcinogen” by the National Toxicology Program [2]. Evidence of

Address Correspondence To: Lawrence H. Lash, Ph.D. Department of Pharmacology Wayne State University School of Medicine 540 East Canfield Avenue Detroit, MI 48201 T: 313-577-0475 F: 313-577-6739 E-mail: l.h.lash@wayne.edu.

Publisher's Disclaimer: This is a PDF file of an unedited manuscript that has been accepted for publication. As a service to our customers we are providing this early version of the manuscript. The manuscript will undergo copyediting, typesetting, and review of the resulting proof before it is published in its final citable form. Please note that during the production process errors may be discovered which could affect the content, and all legal disclaimers that apply to the journal pertain.

the continued interest in the toxicity and human health risk of TRI is highlighted by a series of recent reviews that summarize current state of knowledge and uncertainties [3-6]. Evaluation of the risk for humans potentially exposed to TRI in either the workplace or due to environmental contamination is complicated by the existence of multiple metabolic pathways, multiple target organs, poor or incomplete exposure data for many epidemiology studies, and sex- and species-dependent differences in sensitivity to toxic effects [3,6,7].

The kidneys are one target organ for TRI, and toxicity and carcinogenicity are linked to metabolism of TRI by the glutathione (GSH) conjugation pathway [3,5,7,8]. Once the GSH conjugate is formed, it is further metabolized to the cysteine conjugate S-(1,2-dichlorovinyl)-L-cysteine (DCVC), which is the penultimate nephrotoxic species and has been the focus of most of the mechanistic studies of TRI-induced nephrotoxicity. Much of our previous knowledge of the mechanism of DCVC-induced renal injury came from studies in isolated proximal tubular (PT) cells, proximal tubules, renal cell lines, or subcellular fractions from renal cortical homogenates from rats, rabbits, and other non-human mammals. DCVC was demonstrated to be a potent cytotoxicant in freshly isolated rat PT (rPT) cells [9] and in LLC-PK1 cells [10], with production of mitochondrial dysfunction as an early effect. Similar studies in isolated mitochondria from rat kidneys showed DCVC to be a potent inhibitor of respiration and several dehydrogenases [11-17]. Changes in mitochondrial Ca^{2+} ion homeostasis also appear to be a key step in DCVC-induced renal toxicity [13,18-20]. The importance of mitochondria in DCVC-induced renal toxicity is further highlighted by findings that preservation of mitochondrial function is associated with recovery and repair of epithelial cells from rabbit proximal tubules after sublethal injury from DCVC [21-25]. Other studies in primary cultures of rPT cells, which enable assessment of longer term exposures at lower concentrations as compared to studies that can be conducted in suspensions of freshly isolated cells, showed that DCVC primarily caused necrosis at relatively high concentrations but that concentrations as low as 10 μM increased expression of vimentin [26]. Vimentin is a mesenchymal cell marker that is only expressed in dedifferentiated PT cells that are either undergoing neoplastic transformation or are part of a repair and proliferation process [27-29].

Despite these advances in our understanding of mechanisms of action of DCVC in renal injury, extrapolation of these findings to human kidney involves uncertainties because of species differences in metabolism, transport, and overall susceptibility to injury [3-5,7,8]. To solve the problems inherent in interspecies extrapolation, one approach has been to conduct studies in freshly isolated and primary cultures of human PT (hPT) cells. Comparisons with results obtained with rPT cells showed clear species differences in sensitivity and mode of action. For example, freshly isolated hPT cells exhibit significant release of lactate dehydrogenase (LDH) only at DCVC concentrations above 0.5 mM [30], indicating much lower sensitivity to DCVC than rPT cells. Additionally, whereas acute cytotoxicity induced by DCVC in rPT cells could be substantially prevented by inhibition of the cysteine conjugate β -lyase with aminooxyacetic acid [9] and partially prevented by inhibition of the flavin-containing monooxygenase with methimazole [31], acute cytotoxicity of DCVC in hPT cells was not prevented by aminooxyacetic acid but was significantly diminished by methimazole [30]. This suggests that the two bioactivation enzymes for DCVC play quantitatively different roles in rat and human kidney.

Mechanistic studies on the responses of hPT cells to DCVC revealed many of the same effects as observed in rPT cells, including necrosis, apoptosis, repair, proliferation, and mitochondrial dysfunction [32-34]. Although it is clear that, like in rPT cells, mitochondria are early and prominent intracellular targets of DCVC in hPT cells, we do not know whether induction of mitochondrial dysfunction is obligatory for subsequent cytotoxicity or whether other mechanisms are important in the various responses of hPT cells to DCVC. Hence, in the present study we compared effects of DCVC on necrosis, apoptosis, and proliferation with those on

mitochondrial function. The ability of mitochondrial inhibitors to alter cellular responses to DCVC was assessed to provide more insight into the relationship between mitochondrial effects and cellular responses. The results suggest that in hPT cells, mitochondrial dysfunction is indeed an obligatory step that precedes many of the diverse responses to DCVC.

2. Materials and Methods

2.1. Experimental design

Assessments of time and concentration dependence of DCVC-induced cytotoxicity and proliferation were first conducted to enable placement of the mitochondrial function studies in the proper context with respect to the ultimate cellular response, as the overall goal was to determine the tightness of coupling between cytotoxicity and mitochondrial dysfunction. While our incubations of hPT cells typically use DCVC concentrations of 10 μM through 500 μM , we also measured time- and concentration-dependent effects of DCVC on DNA and protein synthesis with DCVC concentrations of 1 μM and 5 μM , to determine if changes in cellular functions could be observable at lower concentrations. The higher concentrations of DCVC that were used (i.e., 50 to 500 μM) were intended to provide a more complete range of cellular responses.

Although data on potential concentrations of DCVC within PT cells is lacking, there are published data suggesting that the PT cell can be exposed to DCVC under various exposure conditions at concentrations that include at least the lower range of values (i.e., up to 50 μM) that were used in the present study. Humans exposed to relatively low levels of TRI by inhalation (i.e., 100 ppm) transiently exhibit as high as 50 μM concentrations of the GSH conjugate of TRI, *S*-(1,2-dichlorovinyl)glutathione (DCVG), in the plasma [35] and rats exposed to TRI by oral gavage exhibit renal cortical concentrations of DCVC as high as 50 pmol/g tissue [36]. These data suggest that under typical environmental exposure conditions (< 5 ppb), even the lowest concentration of DCVC that was tested (i.e., 1 μM) would be high. Under conditions of exposure to higher concentrations of TRI, such as might occur in occupational exposures and accidental poisonings, intracellular concentrations of DCVC in the PT cell as high as 20 to 50 μM may, at least transiently, be readily achievable.

Mitochondrial function was assessed by measurement of succinate-dependent State 3 oxygen consumption, membrane potential, and cellular ATP content. To assess whether renal cellular injury can occur without mitochondrial dysfunction, DCVC-induced effects were also measured in the presence of agents that specifically prevent processes within the mitochondria that are associated with toxic events. Thus, cyclosporine A (CsA) was used to block the mitochondrial membrane permeability transition (MPT), ruthenium red (RR) was used to inhibit the calcium uniporter, thereby preventing calcium ion cycling, and PK11195 [1-(2-chlorophenyl)-*N*-(1-methylpropyl)-3-isoquinoline-carboxamide] was used as an antagonist of the mitochondrial or peripheral benzodiazepine receptor (mBzR), which is a component of the permeability transition pore. Whereas protection from mitochondrial dysfunction and cell injury by CsA has been used as a marker for involvement of the MPT for many years [37], CsA is also known to cause renal tubular cell apoptosis [38]. In the present study, as in the original work demonstrating inhibition of the MPT [37], we used a CsA concentration of 0.5 nmol/mg protein. Taking into account the amount of cells and volumes used in the assays with CsA and that 1×10^6 hPT cells has about 1 mg of protein [30,32], the concentration of CsA used here to assess the role of the MPT in DCVC-induced cytotoxicity was approximately 0.8 μM . In contrast, Justo et al. [38] demonstrated renal tubular cell apoptosis at CsA concentrations of 0.8 to 8 mM, which is three-to four-orders of magnitude higher than the concentration used here. Hence, CsA-induced cytotoxicity was not a confounding effect in the present studies. Muscarella and colleagues [39] showed that antagonism of the mBzR with PK11195 leads to loss of mitochondrial membrane potential, release of apoptogenic factors,

and exacerbation of cell injury. Hence, the expectation if mitochondrial dysfunction is an obligatory component of DCVC-induced cell injury in hPT cells is that CsA and RR will protect and PK11195 will exacerbate cell injury. Activities of two types of caspases, one whose activation is associated with the mitochondrial pathway of apoptosis (i.e., caspase-3/7) and one whose activation is associated with the non-mitochondrial or extrinsic pathway of apoptosis (i.e., caspase-8) [40], were also measured. Finally, expression of the Fas receptor (FasR), which can be induced in the extrinsic pathway of apoptosis, was also measured by Western blot analysis.

2.2. Chemicals and reagents

TRI was purchased from Sigma Chemical Co. (St. Louis, MO; Cat. No. T4928, ACS reagent, > 99.5% purity). DCVC was synthesized from TRI and L-cysteine in sodium metal and liquid ammonia as described previously [41]. Purity (> 95%) was assessed by HPLC and thin layer chromatography and confirmed by GC-MS. Antimycin A (AA), CsA, PK11195, RR, *tert*-butyl hydroperoxide (tBH), cisplatin (CisPt), methyl vinyl ketone (MVK), anisomycin (Anis), staurosporine (Sts), and lipopolysaccharide (LPS) were purchased from Sigma Chemical Co. The antibody for actin (Sigma) was a polyclonal rabbit antibody that detects the 42-kDa protein in all mammalian species tested, including humans. All other chemicals for cell isolation and culture and for various assays were purchased from commercial vendors and were of the highest purity available.

2.3. Isolation and primary culture of hPT cells

hPT cells were isolated from fresh human kidneys by a modification of the procedure described by Todd et al. [42] as described previously [30,32-34,43]. Cells were identified as being derived from the proximal tubules by their high activities of brush-border membrane enzymes (i.e., alkaline phosphatase and γ -glutamyltransferase) and low activity of the glycolytic enzyme hexokinase, as described previously [9,26,30-34,43,44]. Human kidneys were purchased from Life Legacy Foundation (Tucson, AZ; formerly International Bioresearch Solutions) or the International Institute for the Advancement of Medicine (Edison, NJ). Donor kidneys were obtained with informed consent and all procedures were approved by the Human Investigation Committee of Wayne State University and judged to qualify for Exemption Category 4 according to the criteria used by the Department of Health and Human Services. Kidney tissue was determined to be normal by a pathologist (i.e., derived from non-cancerous, non-diseased tissue) and was screened for HIV, hepatitis A, B, and C, and CMV. Kidneys were perfused with Wisconsin medium and kept on wet ice until they arrived at the laboratory, which was within 24 hr of removal from the donor. Age, gender, and race information, but no other identifying information, was obtained. Because tissue was generally obtained from accident victims or those who have died from cardiovascular incidents and the tissue was rejected for use in transplants (generally because of excessive glomerulosclerosis or arterial plaque), we restricted our donors to adults (age \geq 21 years).

All buffers were continuously bubbled with 95% O₂/5% CO₂ and were maintained at 37°C. Minced cortical pieces from whole kidneys were subjected to collagenase digestion for 60 min, after which the supernatant was filtered through a 70- μ m mesh filter to remove tissue fragments, centrifuged at 150 \times g for 7 min, and the pellet resuspended in Dulbecco's Modified Eagle's Medium : Ham's F12 Medium (DMEM:F12; 1:1). Approximately 5 to 7 \times 10⁶ cells were obtained per 1 g of human kidney cortical tissue. Only cells that excluded > 90% trypan blue or exhibit < 10% leakage of LDH were used for subsequent primary culture. Basal medium and supplements for hPT primary culture were as described previously [32-34,43]. Basal medium was a DMEM:F-12 (1:1) without serum. Medium was supplemented with 15 mM HEPES, pH 7.4, 20 mM NaHCO₃, antibiotics for Day-0 through Day-3 only (192 IU penicillin G/ml + 200 μ g streptomycin sulfate/ml) to inhibit bacterial growth, 2.5 μ g amphotericin B/ml

to inhibit fungal growth, 5 μg bovine insulin/ml (= 0.87 μM), 5 μg human transferrin/ml (= 66 nM), 30 nM sodium selenite, 100 ng hydrocortisone/ml (= 0.28 μM), 100 ng epidermal growth factor/ml (= 17 nM), and 7.5 μg 3,3',5-triiodo-DL-thyronine/ml (= 111 nM). Medium was prepared from powder using doubly-distilled, deionized water. Before addition of supplements, medium was filtered through 0.22- μm porosity cellular acetate membrane filters for sterilization.

hPT cells were seeded (= Day 0) at densities of 1×10^6 cells/ml on Vitrogen-coated, 35-mm dishes, polystyrene culture flasks (T-25 or T-75), or 6- or 24-well plates, depending on the needs of the experiment. Volumes were 1.5 ml, 3 ml, 11 ml, and 1 or 0.5 ml per well for 35-mm dishes, T-25 flasks, T-75 flasks, and 6- or 24-well plates, respectively. Cultures were grown at 37°C in a humidified incubator under an atmosphere of 95% air/5% CO₂ at pH 7.4. After 24 hr (= Day-1), dishes, flasks, or plates were washed with media to remove unattached cells (generally 50 to 60%, based on protein content in dishes and media; [32]) and fresh medium was added. Medium was changed every two days thereafter until confluence (generally by Day 4-6). After Day-3, antibiotics were omitted from medium as they inhibit growth. When necessary, cells were harvested from dishes by either scraping the plates with a Teflon scraper or by brief treatment with Cellstripper (Cellgro, Herndon, VA) (in Ca²⁺- and Mg²⁺-free Hanks' buffer). All experiments were performed with confluent cells.

2.4. Measurement of necrosis by LDH release

Cell death by necrosis was determined by measurement of LDH release from cells. LDH activity was determined in media and, after removal of media, washing of cells with PBS, and solubilization of cells with 0.1% (v/v) Triton X-100, in total cells, by addition of pyruvate and NADH and following the decrease in A₃₄₀. The fraction of LDH release was calculated by the formula: % LDH release = [LDH activity in media/(LDH activity in media + LDH activity in total cells)] \times 100%.

2.5. Flow cytometry and cell cycle analysis

Cell cultures were washed twice with sample buffer (PBS plus glucose (1 g/l) filtered through a 0.22- μm filter), dislodged by treatment with Cellstripper, centrifuged at $400 \times g$ for 10 min, and resuspended in sample buffer. Cell concentrations were adjusted to 1 to 3×10^6 cells/ml with sample buffer and 1 ml of cell suspension was centrifuged at $400 \times g$ for 10 min. All of the supernatant except 0.1 ml/ 10^6 cells was removed and the remaining cells were mixed on a vortex mixer in the remaining fluid for 10 sec. Next, 1 ml of ice-cold ethanol (70%, v/v) was added to the sample drop by drop, with samples being mixed for 10 sec between drops. The tubes were capped and fixed in ethanol at 4°C. After fixation, cells were stained in propidium iodide (50 $\mu\text{g}/\text{ml}$) containing RNase A (100 U/ml). Samples were then mixed, centrifuged at $1,000 \times g$ for 5 min and all the ethanol except 0.1 ml was removed. Cells were mixed in the residual ethanol and 1 ml of the propidium iodide staining solution was added to each tube. After mixing again, cells were incubated at room temperature for at least 30 min. Samples were analyzed within 4 hr by flow cytometry using a Becton Dickinson FACSCalibur Flow Cytometer, which is a core facility of the NIEHS Center for Molecular Toxicology with Human Applications at Wayne State University. Analysis was performed with 20,000 events per sample using the ModFit LT v. 2 for Macintosh data acquisition software package (Verity Software House, Inc., Topsham, ME; distributed by Becton Dickinson Immunocytometry System BDIS, San Jose, CA). Propidium iodide was detected by the FL-2 photomultiplier tube. Fractions of apoptotic cells were quantified by analysis of the sub-G₁ (sub-diploid) peak with ModFit cell cycle analysis. The percent distribution of cells in the various stages of the cell cycle (G₀/G₁, S, G₂/M) were also calculated. Cell aggregates were discarded in the flow cytometry analysis by post-fixation aggregate discrimination.

2.6. Measurement of cell proliferation by MTT assay

Cell proliferation and cytotoxicity were measured by the MTT (3-(4,5-dimethylthiazol-2-yl)-2,5-diphenyltetrazolium bromide) Cell Proliferation Assay kit (ATCC, Manassas, VA) and was expressed in treated samples as the percent of control measurements. Cells were grown on collagen-coated, 24-well plates and incubated with the indicated concentration of DCVC for 4 or 24 hr. At the end of the incubation period, media were replaced with fresh media and the MTT reagent was added to each well. Cells were periodically viewed under a phase contrast microscope for the appearance of the intracellular punctate purple precipitate. Once the precipitate was clearly visible, detergent was added to lyse cells and the plate was incubated in the dark for at least 2 hr, after which time the absorbance at 570 nm was measured in a SpectraMax 2 plate reader (Molecular Devices, Sunnyvale, CA).

2.7. Confocal microscopy

hPT cells were grown on collagen-coated, 35-mm culture dishes and were viewed with a Zeiss Triple-Laser Scanning Confocal Microscope (LSM 310) with integrated workstation at the Confocal Imaging Core Facility in the School of Medicine at Wayne State University (Detroit, MI). This is a core facility of the NIEHS Center for Molecular Toxicology with Human Applications at Wayne State. Initial magnification was 196X.

2.8. Measurement of DNA and protein synthesis

DNA or protein synthesis was quantified by measurement of incorporation of radiolabeled dTTP or L-leucine, respectively, into the acid-insoluble fraction of cell cultures. hPT cells grown on 24-well plates were rinsed with PBS, fresh Krebs-Henseleit buffer (118 mM NaCl, 4.8 mM KCl, 0.96 mM KH_2PO_4 , 0.12 mM $\text{MgSO}_4 \cdot 7\text{H}_2\text{O}$, 25 mM HEPES), containing 225 μM dCTP, dATP, and dGTP was added to each flask, and reaction were initiated by addition of 0.5 $\mu\text{Ci/ml}$ of [methyl- ^3H]-dTTP (70 Ci/mmol; ICN Biomedicals, Inc., Irvine, CA) for measurement of DNA synthesis. For measurement of protein synthesis, deoxynucleotides were omitted from the buffer and reactions were initiated by addition of 0.5 $\mu\text{Ci/ml}$ of [4,5- ^3H]-L-leucine (120 Ci/mmol; Moravak Biochemicals, Brea, CA). Incubations were performed at 37°C in a humidified incubator under an atmosphere of 95% air/5% CO_2 for up to 24 hr. Buffers were then removed, dishes rinsed three times with ice-cold PBS to remove residual radioactivity, and the cells were scraped into 1 ml PBS. Of the 1-ml mixture, 200 μl was removed for determination of total DNA and protein contents. Trichloroacetic acid (265 μl of 30%, w,v) was added to the remaining 800 μl . Cells were then centrifuged for 2 min at 13,000 $\times g$ and the resulting acid-insoluble pellet was dissolved in 0.2% (v/v) Triton X-100 in 1 M NaOH, and aliquots were removed for liquid scintillation counting.

2.9. Assays of mitochondrial function

2.9.1. Mitochondrial respiration—Confluent, primary cultures of hPT cells were grown on collagen-coated T-25 flasks. Cells were incubated for various times up to 48 hr with either PBS or the indicated concentration of DCVC. At the end of the incubation period, cells were released from the culture surface by brief treatment with Cellstripper and resuspended in PBS at a concentration of 2×10^6 cells/ml. Succinate-stimulated O_2 consumption was measured in a Gilson 5/6H Oxygraph as described previously [9,44].

2.9.2. Mitochondrial membrane potential ($\Delta\psi$) measured with JC-1—

Mitochondrial membrane potential ($\Delta\psi$) was measured with the fluorescent agent JC-1 (5,5', 6,6'-tetrachloro-1,1',3,3'-tetraethyl-benzoimidazolylcarbocyanine iodide; Molecular Probes, Eugene, OR) [45,46]. Cells were grown in 6-well plates. Following incubation with the appropriate concentration of toxicant, JC-1 was added to each well at a final concentration of 5 $\mu\text{g/ml}$ and cells were then incubated at 37°C for 30 min. Cells were then washed and viewed

on a confocal microscope using an emission wavelength of 590 nm for the presence of punctate orange-red fluorescence, which indicates polarized mitochondria. In contrast, a diffuse red staining indicates a depolarized mitochondria.

2.9.3. Cellular ATP content—ATP content was quantified by the Cell Titer-Glo Luminescent Cell Viability Assay kit (Promega, Madison, WI) and was expressed in treated samples as the percent control. Standard curves with authentic ATP were generated so that luminescence could be equated to ATP concentration. Cells were grown on collagen-coated, 6-well plates and incubated with the appropriate toxicant dissolved in media for 4 or 24 hr. The cells were washed and scraped into 100 μ l of PBS and then 100 μ l of Cell Titer-Glo reagent was added. The mixture was incubated for 30 min in the dark and the luminescence was read in a SpectraMax 2 plate reader (Molecular Devices).

2.10. Measurement of caspase activities

Activity of caspases-3/7 and -8 were measured by the Caspase Glo 3/7 kit and Caspase Glo 8 kit, respectively (Promega) and cellular caspases-3/7 or -8 activity in treated cells was expressed as the percent of control. Cells were grown on collagen-coated, 6-well plates and incubated with toxicant for 4 or 24 hr. Cells were washed and scraped in 100 μ l PBS and then 100 μ l of Caspase-Glo 3/7 or Caspase-Glo 8 reagent was added. The mixture was then incubated for 2 hr in the dark and the multi-well plate was read in the luminescence mode in a SpectraMax 2 plate reader (Molecular Devices).

2.11. Measurement of FasR expression by Western blot analysis

Total cellular protein (150 μ g) was loaded in wells of 10% polyacrylamide gels. After electroblotting of protein onto nitrocellulose paper, blots were blocked for 1 hr in 5% milk powder solution and incubated overnight with the primary antibody to the FasR. The antibody was a polyclonal antibody made in rabbit that recognizes the human FasR protein (molecular weight 48 kDa) and was purchased from Santa Cruz Biotechnology (Santa Cruz, CA). Blots were then washed three times with Tris-buffered saline containing Tween-20 (TTBS) and incubated with a secondary antibody conjugated to alkaline phosphatase (Jackson ImmunoResearch, West Grove, PA) for 1 hr. Blots were washed 3-6 times and then assayed for color development using BCIP/NBT as substrates (Promega, Madison, WI). Alkaline phosphatase staining intensity was determined by scanning laser densitometry with a Fuji Science Imaging System connected to a Macintosh G4 computer.

2.12. Data analysis

Data values for experiments involving measurements of ATP content, caspase activities, respiratory activity, and DNA content were normalized to cellular protein content. Protein was measured using the bicinchoninic acid protein assay kit (Pierce, Rockford, IL) and measuring absorbance at 562 nm. Standard curves using bovine serum albumin as the standard were generated to determine sample protein concentrations. Significant differences between mean values of controls and treated samples were first assessed by a one-way or two-way analysis of variance. When significant *F* values were obtained with the analysis of variance, the Fisher's protected least-significance *t* test was performed to determine which means were significantly different from one another, with two-tail probabilities < 0.05 considered significant.

3. Results

3.1. Cytotoxicity, proliferation, and morphology

To place mitochondrial dysfunction into the context of cytotoxicity, confluent, primary cultures of hPT cells were incubated for either 4 hr or 24 hr with DCVC, ranging in concentrations from

10 μM to 300 μM . We first assessed release of LDH as an index of necrosis (Figure 1). Incubation with 10 μM DCVC had no effect on LDH release at either time point. In contrast, incubation with DCVC concentrations of 50 μM and higher caused both a time- and concentration-dependent increase in LDH release, with a maximum level of LDH release of approximately 27%.

Assessment of toxicity and proliferation capacity by the MTT assay gave generally similar results as the LDH release assay, except that in this case, 10 μM DCVC did elicit significant effects (Figure 2). No cell proliferation was observed at the 4-hr incubations; rather, a DCVC concentration-dependent decrease in MTT reduction occurred, with the highest concentration tested (300 μM), reducing MTT reduction by approximately 40%. In contrast, DCVC concentrations as low as 10 μM significantly increased MTT reduction at 24 hr, suggesting enhanced cell proliferation. As DCVC concentrations were increased, however, the increase in MTT reduction was diminished and was lower than control cells at 300 μM , suggesting cytotoxicity. Because MTT reduction occurs in mitochondria, the decreases with increasing DCVC concentrations are consistent with mitochondrial dysfunction.

Flow cytometry analysis of propidium iodide-stained hPT cells was used to assess the occurrence of apoptosis and the fraction of cells that were in the S phase, indicative of proliferating cells (Figure 3). DCVC concentrations as low as 10 μM significantly increased apoptosis at both 4 hr and 24 hr exposures; apoptosis was maximal at 50 μM DCVC and was greater at 4 hr than at 24 hr exposures. The extent of apoptosis decreased at higher concentrations of DCVC and no apoptosis was observed at 300 μM DCVC. As we concluded previously [29-31], the decrease in the amount of apoptosis detected with higher concentrations of DCVC and/or after longer exposure periods is likely due to a greater amount of necrosis in these cell populations. Significant, but modest cell proliferation, as assessed by increases in the proportion of cells in S phase, was only observed at 10 μM DCVC and a 4-hr exposure. The proportion of cells in S phase decreased at 24-hr exposures at concentrations ≥ 200 μM DCVC.

As an example of effects of DCVC on cellular morphology, time-dependent effects of 50 μM DCVC were assessed by phase contrast microscopy (Figure 4). We chose 50 μM as the concentration of DCVC because this was the concentration that produced maximal amounts of apoptosis but only small increases in LDH release. Little change in cellular morphology was observed after a 4-hr incubation with 50 μM DCVC. With increasing incubation time, however, progressive alterations in cellular morphology were observed, as indicated by increases in formation of intracellular vesicles, loss of cuboidal epithelial shape, and increasing amounts of debris.

As a potentially more sensitive indicator of cell function, we measured amounts of DNA and protein in hPT cells incubated for up to 24 hr with between 1 μM and 50 μM DCVC, to derive rates of DNA and protein synthesis (Figure 5). Rates of DNA synthesis increased approximately 5- to 6-fold over the time course of culture, reaching maximal levels at 4 hr and decreasing slightly at 6 hr and 24 hr. Based on DNA synthesis rates, there was no evidence of net proliferation at DCVC concentrations up to 50 μM . Although rates of protein synthesis also tended to increase with time in culture, the increases were more gradual (i.e., maximal at 24 hr) and modest (approximately 2-fold). Exposure to 25 μM DCVC significantly increased rates of protein synthesis at 4, 6, and 24 hr, suggesting some promotion of proliferation.

3.2. DCVC-induced mitochondrial dysfunction

As a basic assessment of mitochondrial function, succinate-dependent oxygen consumption was measured in hPT cells incubated for up to 48 hr with media (= Control), DCVC (10 - 500 μM), or Sts (Figure 6). Succinate-dependent respiration was maintained over 48 hr of culture

in control cells but decreased in a time- and concentration-dependent manner in cells incubated with 10 μM to 500 μM DCVC. Besides increasing with increasing DCVC concentration, the extent of inhibition of respiration markedly increased with time; for example, whereas 100 μM DCVC only produced about 25% inhibition at 1 hr, it produced 38% inhibition at 4 hr, 50% inhibition at 8 hr, 65% inhibition at 24 hr, and 80% inhibition at 48 hr. For comparison, the effect of 1 μM Sts, as a control for an agent that produces apoptosis, was determined. Sts produced no effect on respiration at 1 and 2 hr, only 25% inhibition at 4 hr, 50% inhibition at 8 and 24 hr, and about 65% inhibition at 48 hr. This delayed time course suggests that Sts-induced apoptosis occurs primarily at a time when Sts does not significantly affect mitochondrial function (i.e., ≤ 4 hr).

We next determined cellular ATP concentrations in hPT cells treated for 24 hr with either DCVC (10 to 300 μM) or several positive and negative controls (Table 1). DCVC caused a progressive decrease in ATP contents: At concentrations at which significant apoptosis occurs (≤ 200 μM), no more than 40% depletion of ATP was observed; at a higher concentration of DCVC that is primarily necrotic rather than apoptotic, ATP depletion was $> 50\%$. By contrast, incubation with 1 mM KCN + 0.1 mM iodoacetate (KCN/IAA) or 50 μM tBH produced approximately 80% ATP depletion, whereas 1 μM AA or 1 μM Sts only produced approximately 20% ATP depletion.

The influence of DCVC on caspase activities was assessed as another indicator of the involvement of mitochondria in DCVC-induced toxicity (Table 2). Activation of caspase-3/7 is indicative of apoptosis that occurs through the mitochondrial pathway whereas activation of caspase-8 is indicative of apoptosis that occurs through the extrinsic or extra-mitochondrial pathway. AA had no effect on either caspase-3/7 at 4 hr or 24 hr or caspase-8 at 4 hr, but significantly increased activity of caspase-8 at 24 hr. Sts significantly increased both types of caspases at both time points; effects on caspase-3/7 were greater than those on caspase-8, suggesting that the mitochondrial pathway is more important in Sts-induced apoptosis. At the 4-hr incubation, DCVC produced a significant increase in caspase-3/7 activity at 10 μM and 50 μM and in caspase-8 only at 10 μM ; the increase in caspase-3/7 activity was larger than that in caspase-8 activity, suggesting a greater role for mitochondrial- vs. extramitochondrial-mediated apoptosis. At the 24-hr time point, however, DCVC only increased caspase-8 activity at ≤ 100 μM ; caspase-3/7 activity decreased in a DCVC concentration-dependent manner, suggesting primarily necrosis at later time points and higher concentrations of DCVC.

3.3. Influence of modulation of mitochondrial function on DCVC-induced toxicity

hPT cells were incubated for 2, 6, or 24 hr with 0, 10, 50, or 100 μM DCVC in the absence or presence of the MPT inhibitor CsA (0.5 nmol/mg protein = approximately 0.8 μM), to examine the influence of CsA on DCVC-induced apoptosis (Figure 7). In the absence of CsA, DCVC induced modest amounts of apoptosis as compared to untreated control cells at 2 hr (2.7- to 4.6-fold increase vs. control cells), larger amounts at 6 hr (2.7- to 16.0-fold increase vs. control cells), and modest amounts at 24 hr (2.4- to 9.2-fold increase vs. control cells). CsA significantly decreased DCVC-induced apoptosis at relatively low DCVC concentrations at the 6-hr incubation and at 10 μM DCVC at 24 hr. Thus, at the 2-hr incubation time, DCVC-treated cells increased the number of apoptotic cells only 1.3- to 2.2-fold in the presence of CsA. In contrast, CsA increased apoptosis with 100 μM DCVC at 24 hr (44-fold increase over control with CsA as compared to 16.0-fold increase over control without CsA), which is a time and DCVC concentration at which the primary cellular response is necrosis. Regardless of the complexity of the influence of CsA, the results clearly demonstrate a prominent role for mitochondrial dysfunction and the MPT in the hPT cell response to DCVC.

To determine the effect of DCVC and mitochondrial inhibitors on mitochondrial $\Delta\psi$, we first assessed effects of several mitochondrial inhibitors to provide a basis for comparison and to

validate the assay in the primary cultures of hPT cells. Control hPT cells exhibited red punctate fluorescence, indicative of maintenance of a high $\Delta\psi$ (Figure 8A). In contrast, incubation of cells with AA resulted in a complete loss of $\Delta\psi$, as would be expected of this inhibitor (Figure 8B). Incubation with the MPT inhibitor CsA had a minimal effect on $\Delta\psi$ (Figure 8C), suggesting that mitochondrial function is maintained. Similarly, the Ca^{2+} -uniporter inhibitor ruthenium red (RR) also resulted in maintenance of $\Delta\psi$, which again is expected based on the ability of this chemical to prevent futile cycling of Ca^{2+} ions, which would lead to a dissipation of $\Delta\psi$ (Figure 8D). Co-incubation of hPT cells with AA and CsA resulted in some restoration of $\Delta\psi$ (Figure 8E), again consistent with inhibition of the MPT leading to preservation of mitochondrial function. Co-incubation of hPT cells with AA, the peripheral benzodiazepine receptor (pBzR) inhibitor PK11195, and CsA also resulted in some restoration of $\Delta\psi$ (Figure 8F), consistent with inhibition of the MPT and Ca^{2+} cycling leading to preservation of mitochondrial function, although the preservation appeared to be somewhat less than that with AA and CsA alone. In contrast, hPT cells co-incubated with RR and PK11195 exhibited virtually no JC-1 fluorescence (Figure 8G), indicating that simultaneous inhibition of Ca^{2+} uptake and the pBzR results in inhibition of mitochondrial function.

In comparison with control hPT cells (Figure 9A), cells incubated for 4 hr with 50 μM DCVC exhibited modestly decreased intensity of JC-1 fluorescence (Figure 9B), suggesting a modest decrease in $\Delta\psi$, which is consistent with the modest ATP depletion (cf. Table 1). Co-incubation of hPT cells for 4 hr with 50 μM DCVC and CsA resulted in some maintenance of JC-1 fluorescence (Figure 9C), consistent with modest protection. In contrast, co-incubation of hPT cells for 4 hr with 50 μM DCVC and PK11195 resulted in an almost complete loss of JC-1 fluorescence (Figure 9D), suggesting that inhibition of the pBzR exacerbates DCVC-induced mitochondrial dysfunction. As with CsA, co-incubation of hPT cells for 4 hr with 50 μM DCVC and RR resulted in maintenance of JC-1 fluorescence (Figure 9E), consistent with changes in mitochondrial Ca^{2+} ion homeostasis playing a role in DCVC-induced mitochondrial dysfunction. Finally, co-incubation of hPT cells for 4 hr with 50 μM DCVC and CsA and PK11195 resulted in an almost complete loss of JC-1 fluorescence (Figure 9F), suggesting that inhibition of the pBzR abrogates or prevents the protective effect of CsA.

3.4. FasR expression

To further investigate whether DCVC-induced apoptosis in hPT cells can also occur through a non-mitochondrial mechanism, we determined expression of FasR after 4-hr incubations with either model chemicals or DCVC or its parent molecule, TRI (Figure 10). While 50 μM tBH had no effect, 100 μM CisPt decreased and 100 μM MVK increased FasR expression (Figure 10A). Because we have shown that tBH is a potent mitochondrial toxicant in renal PT cells [47-49], the absence of FasR induction is consistent with it producing either necrosis or apoptosis through the mitochondrial pathway. MVK, however, did modestly increase FasR expression, consistent with it acting through both a mitochondrial and extra-mitochondrial mechanism [50]. Anis and Sts were also tested as controls: Anis is a non-selective mitogen-activated protein kinase inhibitor [51] and Sts is a protein kinase inhibitor that is frequently used as a positive control for inducing apoptosis and produces apoptosis in primary cultures of hPT cells [32]. Anis slightly decreased whereas Sts had no apparent effect on FasR expression.

Neither DCVC nor its parent molecule TRI significantly altered FasR expression (Figure 10B), suggesting little involvement of the extrinsic pathway in DCVC-induced apoptosis. hPT cells were also exposed to 1 $\mu\text{g}/\text{ml}$ LPS as a positive control for induction of FasR. FasR expression was only slightly higher in LPS-treated cells at 4 hr but was lower at 24 hr, suggesting that this pathway does not function well in these hPT cell cultures (data not shown). The decrease in FasR expression at 24 hr with LPS treatment is likely due to LPS-induced cytotoxicity.

4. Discussion

The objective of the present work was to assess the importance of mitochondrial dysfunction in the mechanisms by which hPT cells respond to DCVC exposure. The hypothesis that was tested is that mitochondrial dysfunction is a critical and necessary step in DCVC-induced cytotoxicity. Indeed, results of the present study confirm that exposure of hPT cells to DCVC elicits necrosis, apoptosis, and a modest degree of proliferation, that the extent of these responses varies depending on DCVC concentration and exposure time, and that mitochondrial dysfunction occurs at an early time after the initial exposure. Moreover, inhibition of key mitochondrial processes significantly modulated the cytotoxic responses to DCVC, supporting the hypothesis that mitochondrial dysfunction is an obligatory step.

In our earlier studies on DCVC-induced necrosis, apoptosis, and proliferation in hPT cells [32,34], we found that, depending on exposure time and the process being measured, the lowest DCVC concentration at which we could detect significant changes in hPT cells was 10 μM for some processes but was 50 μM or higher for others. For LDH release (cf. Figure 1), 50 μM DCVC was the lowest concentration that had a significant effect, although the effect was quite modest. For MTT fluorescence and cell cycle analysis (cf. Figures 2 and 3), significant changes were detected at 10 μM DCVC. Decreases in MTT fluorescence are often taken to imply cytotoxicity, but are also influenced by loss of mitochondrial energization, which can occur without or prior to cell death. Using rates of DNA and protein synthesis as a potentially more sensitive indicator of cytotoxicity or proliferation, however, small and statistically significant changes were observed with 1 μM and 5 μM DCVC. Importantly, evidence of DCVC-induced proliferation, although modest in scope, was only observed at the lowest concentrations tested. Cytotoxicity becomes more prominent at higher concentrations (cf. Figure 1), making the cells incompetent to undergo repair and proliferation.

The prominence and potency of the mitochondria as intracellular targets and sites of action are evident from examination of the time- and concentration-dependent effects of DCVC on succinate-dependent respiration (cf. Figure 6). As found previously in hPT cells [32-34], rPT cells [9,12-15,17-20,26,31], and rabbit proximal tubules [21-25], hPT cells in the current study exhibited decreases in respiration. Modest effects were observed at 10 μM DCVC and none were detected at 1 or 5 μM DCVC. Sts, a broad-specificity protein kinase inhibitor that we have used previously as a positive control for inducing apoptosis [32], was a modest inhibitor of respiration, consistent with the need for some cellular energy for undergoing apoptosis. Similar findings were observed with measurements of cellular ATP contents. Both Sts and DCVC concentrations that produce primarily apoptosis in hPT cells, produced only modest depletion of ATP, in contrast with tBH and IAA/KCN, which caused > 75% depletion of ATP. This contrasts with the much larger decreases observed in respiration rates, suggesting that the hPT cell responds to the initial toxic insult by down-regulating ATP consumption to preserve ATP stores.

Examination of effects on two types of caspase activities, caspase-3/7 and caspase-8, whose activation are associated with the mitochondrial and extrinsic pathways of apoptosis, respectively, provided additional evidence consistent with the former and not the latter pathway being the predominant one involved in DCVC-induced apoptosis. DCVC concentrations ≥ 100 μM , particularly at the 24-hr time point, were associated with significant inhibition of caspase activity, presumably due to the increasing extent of cell death. The relatively modest amounts of activation and differences between responses of the two types of caspases preclude a clear conclusion, based on these data alone, about the role of the two pathways in DCVC-induced apoptosis.

To assess further whether mitochondrial involvement in the mechanism of action of DCVC is obligatory, selected parameters of cytotoxicity and mitochondrial function were measured in the presence and absence of inhibitors of specific mitochondrial processes. As expected, CsA and RR, which block the MPT and Ca^{2+} ion cycling, respectively, were both protective, as evidenced by retention of mitochondrial $\Delta\psi$ in DCVC-treated hPT cells. In contrast, the mBzR antagonist PK11195 exacerbated loss of mitochondrial $\Delta\psi$ due to DCVC, consistent with its ability to facilitate opening of the MPT [39]. Effects of CsA on DCVC-induced apoptosis (cf. Figure 7) provided additional insight into the key role of mitochondrial dysfunction in DCVC-induced cytotoxicity. At relatively low DCVC concentrations and/or early exposure times, CsA significantly decreased the extent of apoptosis in hPT cells. At higher DCVC concentrations and/or later exposure times (e.g., 100 μM DCVC at 24 hr; Figure 7C), however, hPT cells pretreated with CsA exhibited higher levels of apoptosis than those incubated with DCVC alone. We interpret this finding by considering the range of cellular responses to represent a continuum, as shown in the scheme in Figure 11. Thus, at the higher dose and later time, CsA protection would be suggested to involve a shift in cellular response from necrosis to apoptosis. At the lower concentrations of DCVC and/or earlier exposure times, we suggest that CsA shifts the cellular response from apoptosis to repair and proliferation.

Although our preliminary conclusion is that the extrinsic pathway of apoptosis induction plays little role for DCVC in hPT cells, based on the smaller increase in activity of caspase-8 vs. caspase-3/7 and the FasR expression measurements, additional work is needed to confirm this and to assess if there are any exposure conditions that could result in a stronger enhancement of the extra-mitochondrial pathway. Additionally, the lack of a robust response in the FasR measurements with LPS suggest that this pathway may not have optimal function in the primary cell cultures, making assessment of its role in toxicity difficult. Thus, although this pathway may have more of a role than indicated here, the available data can be predominantly explained by the mitochondrial pathway.

In conclusion, the initial studies presented here were designed to assess time and concentration dependence of cellular responses to DCVC in primary cultures hPT cells so that mitochondrial dysfunction could be placed in the proper context. The cellular responses involved a range, from repair and proliferation to apoptosis to necrosis. We then tested the hypothesis that mitochondrial dysfunction is an integral and obligatory component of DCVC-induced cytotoxicity. The results support the hypothesis, suggesting that alterations in mitochondrial function are an early event subsequent to DCVC exposure and that cytotoxic responses ensue from that point. Hence, mitochondria can be viewed as the gateway that regulates the cellular response to environmental stresses and pathological states. Strategies to intervene after exposure to DCVC or similar chemicals, designed to prevent irreversible tissue injury, should focus on early steps such as mitochondrial function, to have the broadest applicability.

Acknowledgments

This work was supported by a grant to LHL from the National Institute of Environmental Health Sciences (R01-ES08828). Core facilities funded by the National Institute of Environmental Health Sciences Center for Molecular Toxicology with Human Application (Grant P30-ES06639) at Wayne State University were used for some of these studies. We thank Jan Crowley (Washington University, St. Louis, MO) for the GC-MS analysis of DCVC.

References

- [1]. International Agency for Research on Cancer (IARC). IARC Monogr Eval Carcinog Risks Hum. 63. 1995. Dry cleaning, some chlorinated solvents, and other industrial chemicals; p. 75-158.
- [2]. National Toxicology Program (NTP). Report on Carcinogens. 10th. U.S. Department of Health and Human Services, Public Health Service, National Toxicology Program; Research Triangle Park, NC: 2002.

- [3]. Caldwell JC, Keshava N. Key issues in the modes of action and effects of trichloroethylene metabolites for liver and kidney tumorigenesis. *Environ Health Perspec* 2006;114:1457–1463.
- [4]. Chiu WA, Caldwell JC, Keshava N, Scott CS. Key scientific issues in the health risk assessment of trichloroethylene. *Environ Health Perspec* 2006;114:1445–1449.
- [5]. Lock EA, Reed CJ. Trichloroethylene: Mechanisms of renal toxicity and renal cancer and relevance to risk assessment. *Toxicol Sci* 2006;91:313–331. [PubMed: 16421178]
- [6]. Scott CS, Chiu WA. Trichloroethylene cancer epidemiology: A consideration of select issues. *Environ Health Perspec* 2006;114:1471–1478.
- [7]. Lash LH, Fisher JW, Lipscomb JC, Parker JC. Metabolism of trichloroethylene. *Environ Health Perspec* 2000;108(Suppl 2):177–200.
- [8]. Lash LH, Parker JC, Scott CS. Modes of action of trichloroethylene for kidney tumorigenesis. *Environ Health Perspec* 2000;108(Suppl 2):225–240.
- [9]. Lash LH, Anders MW. Cytotoxicity of S-(1,2-dichlorovinyl)glutathione and S-(1,2-dichlorovinyl)-L-cysteine in isolated rat kidney cells. *J Biol Chem* 1986;261:13076–13081. [PubMed: 2875994]
- [10]. Chen Y, Cai J, Anders MW, Stevens JL, Jones DP. Role of mitochondrial dysfunction in S-(1,2-dichlorovinyl)-L-cysteine-induced apoptosis. *Toxicol Appl Pharmacol* 2001;170:172–180. [PubMed: 11162782]
- [11]. Cooper AJL, Bruschi SA, Anders MW. Toxic, halogenated cysteine S-conjugates and targeting of mitochondrial enzymes of energy metabolism. *Biochem Pharmacol* 2002;64:553–564. [PubMed: 12167474]
- [12]. Lash LH, Elfarra AA, Anders MW. Renal cysteine conjugate β -lyase: Bioactivation of nephrotoxic cysteine S-conjugates in mitochondrial outer membrane. *J Biol Chem* 1986;261:5930–5935. [PubMed: 3700378]
- [13]. Lash LH, Anders MW. Mechanism of S-(1,2-dichlorovinyl)-L-cysteine- and S-(1,2-dichlorovinyl)-L-homocysteine-induced renal mitochondrial toxicity. *Mol Pharmacol* 1987;32:549–556. [PubMed: 3670284]
- [14]. Lash LH, Xu Y, Elfarra AA, Duescher RJ, Parker JC. Glutathione-dependent metabolism of trichloroethylene in isolated liver and kidney cells of rats and its role in mitochondrial and cellular toxicity. *Drug Metab Dispos* 1995;23:846–853. [PubMed: 7493552]
- [15]. Lash LH, Qian W, Putt DA, Hueni SE, Elfarra AA, Krause RJ, Parker JC. Renal and hepatic toxicity of trichloroethylene and its glutathione-derived metabolites in rats and mice: Sex-, species-, and tissue-dependent differences. *J Pharmacol Exp Ther* 2001;297:155–164. [PubMed: 11259540]
- [16]. Stevens JL, Ayoubi N, Robbins JD. The role of mitochondrial matrix enzymes in the metabolism and toxicity of cysteine conjugates. *J Biol Chem* 1988;263:3395–3401. [PubMed: 3343250]
- [17]. van de Water B, Zoetewij JP, de Bont HJGM, Nagelkerke JF. Inhibition of succinate:ubiquinone reductase and decrease of ubiquinol in nephrotoxic cysteine S-conjugate-induced oxidative cell injury. *Mol Pharmacol* 1995;48:928–937. [PubMed: 7476924]
- [18]. Vamvakas S, Bittner D, Dekant W, Anders MW. Events that precede and that follow S-(1,2-dichlorovinyl)-L-cysteine-induced release of mitochondrial Ca^{2+} and their association with cytotoxicity to renal cells. *Biochem Pharmacol* 1992;44:1131–1138. [PubMed: 1417936]
- [19]. van de Water B, Zietbey JP, de Bront HJGM, Mulder GJ, Nagelkerke JF. The relationship between intracellular Ca^{2+} and the mitochondrial membrane potential in isolated proximal tubular cells from rat kidney exposed to the nephrotoxin 1,2-dichlorovinyl-cysteine. *Biochem Pharmacol* 1993;45:2259–2267. [PubMed: 8517866]
- [20]. van de Water B, Zoetewij JP, de Bont HJGM, Mulder GJ, Nagelkerke JF. Role of mitochondrial Ca^{2+} in the oxidative stress-induced dissipation of the mitochondrial membrane potential: Studies in isolated proximal tubular cells using the nephrotoxin 1,2-dichlorovinyl-L-cysteine. *J Biol Chem* 1994;269:14546–14552. [PubMed: 8182062]
- [21]. Liu X, Godwin ML, Nowak G. Protein kinase C-inhibits the repair of oxidative phosphorylation after S-(1,2-dichlorovinyl)-L-cysteine injury in renal cells. *Am J Physiol* 2004;287:F64–F73.
- [22]. Nowak G. Protein kinase C mediates repair of mitochondrial and transport functions following toxicant-induced injury in renal cells. *J Pharmacol Exp Ther* 2003;306:157–165. [PubMed: 12665543]

- [23]. Nowak G, Keasler KB, McKeller DE, Schnellmann RG. Differential effects of EGF on repair of cellular functions after dichlorovinyl-L-cysteine-induced injury. *Am J Physiol* 1999;276:F228–F236. [PubMed: 9950953]
- [24]. Shaik ZP, Fifer EK, Nowak G. Protein kinase B/Akt modulates nephrotoxicant-induced necrosis in renal cells. *Am J Physiol* 2007;292:F292–F303.
- [25]. Shaik ZP, Fifer EK, Nowak G. Akt activation improves oxidative phosphorylation in renal proximal tubular cells following nephrotoxicant injury. *Am J Physiol* 2008;294:F423–F432.
- [26]. Cummings BS, Zangar RC, Novak RF, Lash LH. Cytotoxicity of trichloroethylene and S-(1,2-dichlorovinyl)-L-cysteine in primary cultures of rat renal proximal tubular and distal tubular cells. *Toxicology* 2000;150:83–98. [PubMed: 10996665]
- [27]. Wallin A, Zhang G, Jones TW, Jaken S, Stevens JL. Mechanism of the nephrogenic repair response: Studies on proliferation and vimentin expression after S-(1,2-dichlorovinyl)-L-cysteine nephrotoxicity in vivo and in cultured proximal tubule epithelial cells. *Lab Invest* 1992;66:474–484. [PubMed: 1374823]
- [28]. Ward JM, Stevens JL, Konishi N, Kurata Y, Uno H, Diwan BA, Ohmori T. Vimentin metaplasia in renal cortical tubules of preneoplastic, neoplastic, aging, and regenerative lesions of rats and humans. *Am J Pathol* 1992;141:955–964. [PubMed: 1415487]
- [29]. Witzgall R, Brown D, Schwartz C, Bonventre JV. Localization of proliferating cell nuclear antigen, vimentin, c-Fos, and clusterin in the postischemic kidney: Evidence for a heterogeneous genetic response among nephron segments, and a large pool of mitotically active and dedifferentiated cells. *J Clin Invest* 1994;93:2175–2188. [PubMed: 7910173]
- [30]. Cummings BS, Lash LH. Metabolism and toxicity of trichloroethylene and S-(1,2-dichlorovinyl)-L-cysteine in freshly isolated human proximal tubular cells. *Toxicol Sci* 2000;53:458–466. [PubMed: 10696794]
- [31]. Lash LH, Sausen PJ, Duescher RJ, Cooley AJ, Elfarra AA. Roles of cysteine conjugate β -lyase and S-oxidase in nephrotoxicity: Studies with S-(1,2-dichlorovinyl)-L-cysteine and S-(1,2-dichlorovinyl)-L-cysteine sulfoxide. *J Pharmacol Exp Ther* 1994;269:374–383. [PubMed: 8169843]
- [32]. Lash LH, Hueni SE, Putt DA. Apoptosis, necrosis and cell proliferation induced by S-(1,2-dichlorovinyl)-L-cysteine in primary cultures of human proximal tubular cells. *Toxicol Appl Pharmacol* 2001;177:1–16. [PubMed: 11708895]
- [33]. Lash LH, Putt DA, Hueni SE, Krause RJ, Elfarra AA. Roles of necrosis, apoptosis, and mitochondrial dysfunction in S-(1,2-dichlorovinyl)-L-cysteine sulfoxide-induced cytotoxicity in primary cultures of human renal proximal tubular cells. *J Pharmacol Exp Ther* 2003;305:1163–1172. [PubMed: 12626654]
- [34]. Lash LH, Putt DA, Hueni SE, Horwitz BP. Molecular markers of trichloroethylene-induced toxicity in human kidney cells. *Toxicol Appl Pharmacol* 2005;206:157–168. [PubMed: 15967204]
- [35]. Lash LH, Putt DA, Brashear WT, Abbas R, Parker JC, Fisher JW. Identification of S-(1,2-dichlorovinyl)glutathione in the blood of human volunteers exposed to trichloroethylene. *J Toxicol Environ Health* 1999;56:1–21.
- [36]. Lash LH, Putt DA, Parker JC. Metabolism and tissue distribution of orally administered trichloroethylene in male and female rats: Identification of glutathione- and cytochrome P-450-derived metabolites in liver, kidney, blood, and urine. *J Toxicol Environ Health* 2006;69:1285–1309.
- [37]. Broekemeier KM, Dempsey ME, Pfeiffer DR. Cyclosporin A is a potent inhibitor of the inner membrane permeability transition in liver mitochondria. *J Biol Chem* 1989;264:2826–2830. [PubMed: 2536725]
- [38]. Justo P, Lorz C, Sanz A, Egido J, Ortiz A. Intracellular mechanisms of cyclosporin A-induced tubular cell apoptosis. *J Am Soc Nephrol* 2003;14:3072–3080. [PubMed: 14638906]
- [39]. Muscarella DE, O'Brien KA, Lemley AT, Bloom SE. Reversal of Bcl-2 mediated resistance of the EW36 human B-cell lymphoma cell line to arsenite and pesticide-induced apoptosis by PK11195, a ligand of the mitochondrial benzodiazepine receptor. *Toxicol Sci* 2003;74:66–73. [PubMed: 12730627]

- [40]. Wang X, Ryter SW, Dai C, Tang Z-L, Watkins SC, Yin X-M, Song R, Choi AMK. Necrotic cell death in response to oxidant stress involves the activation of the apoptogenic caspase-8/Bid pathway. *J Biol Chem* 2003;278:29184–29191. [PubMed: 12754217]
- [41]. Elfarra AA, Jakobson I, Anders MW. Mechanism of *S*-(1,2-dichlorovinyl)glutathione-induced nephrotoxicity. *Biochem Pharmacol* 1986;35:283–288. [PubMed: 2867768]
- [42]. Todd JH, McMartin KE, Sens DA, Jones GE. Enzymatic isolation and serum-free culture of human renal cells. *Methods in Molecular Medicine: Human Cell Culture Protocols* 1995 Ed., Chapter 32, Humana Press, Inc. Totowa, NJ
- [43]. Cummings BS, Lasker JM, Lash LH. Expression of glutathione-dependent enzymes and cytochrome P450s in freshly isolated and primary cultures of proximal tubular cells from human kidney. *J Pharmacol Exp Ther* 2000;293:677–685. [PubMed: 10773044]
- [44]. Lash LH, Tokarz JJ. Isolation of two distinct populations of cells from rat kidney cortex and their use in the study of chemical-induced toxicity. *Anal Biochem* 1989;182:271–279. [PubMed: 2692474]
- [45]. Reers M, Smith TW, Chen LB. J-aggregate formation of a carbocyanine as a quantitative fluorescent indicator of membrane potential. *Biochemistry* 1991;30:4480–4486. [PubMed: 2021638]
- [46]. Smiley ST, Reers M, Mottola-Hartshorn C, Lin M, Chen A, Smith TW, Steele GD Jr, Chen LB. Intracellular heterogeneity in mitochondrial membrane potentials revealed by a J-aggregate-forming lipophilic cation JC-1. *Proc Natl Acad Sci USA* 1991;88:3671–3675. [PubMed: 2023917]
- [47]. Lash LH, Putt DA, Matherly LH. Protection of NRK-52E cells, a rat renal proximal tubular cell line, from chemical induced apoptosis by overexpression of a mitochondrial glutathione transporter. *J Pharmacol Exp Ther* 2002;303:476–486. [PubMed: 12388626]
- [48]. Xu F, Putt DA, Matherly LH, Lash LH. Modulation of expression of rat mitochondrial 2-oxoglutarate carrier in NRK-52E cells alters mitochondrial transport and accumulation of glutathione and susceptibility to chemically induced apoptosis. *J Pharmacol Exp Ther* 2006;316:1175–1186. [PubMed: 16291728]
- [49]. Lash LH, Tokarz JJ. Oxidative stress in isolated rat renal proximal and distal tubular cells. *Am J Physiol* 1990;259:F338–F347. [PubMed: 2386209]
- [50]. Lash LH, Woods EB. Cytotoxicity of alkylating agents in isolated rat kidney proximal tubular and distal tubular cells. *Arch Biochem Biophys* 1991;286:46–56. [PubMed: 1897958]
- [51]. Chaturvedi LS, Koul S, Sekhon A, Bhandari A, Menon M, Koul HK. Oxalate selectively activates p38 mitogen-activated protein kinase and c-Jun N-terminal kinase signal transduction pathways in renal epithelial cells. *J Biol Chem* 2002;277:13321–13330. [PubMed: 11823457]

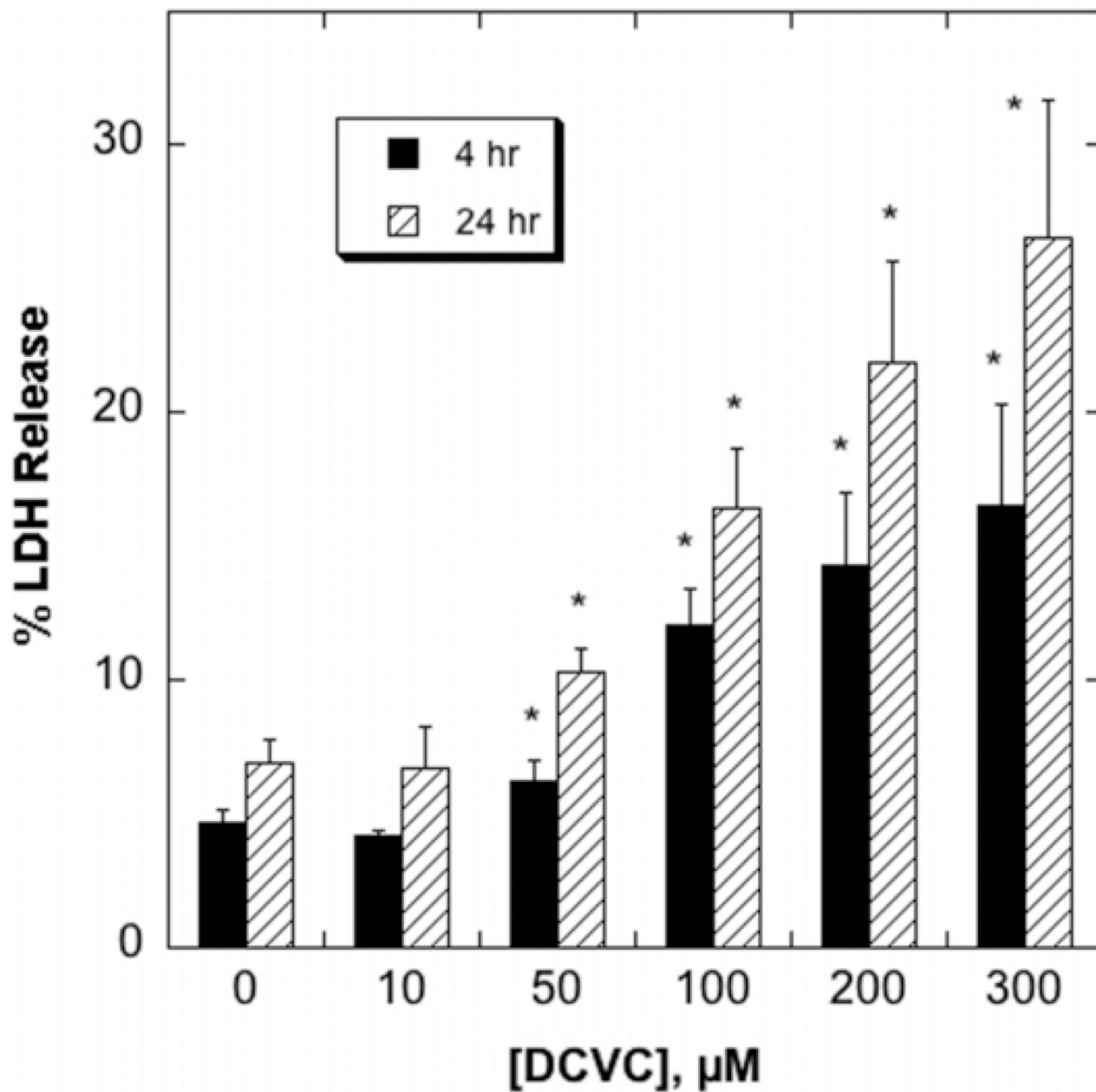


Figure 1.

Figure 1. DCVC-induced necrosis assessed by LDH release

Confluent primary cultures of hPT cells grown in collagen-coated, 6-well plates were incubated for 4 or 24 hr with the indicated concentrations of DCVC. LDH release was measured spectrophotometrically and is expressed as percent release. Data are means \pm SEM of measurements from 4 separate cell cultures, each deriving from a different kidney.

*Significantly different ($P < 0.05$) from the corresponding control cells.

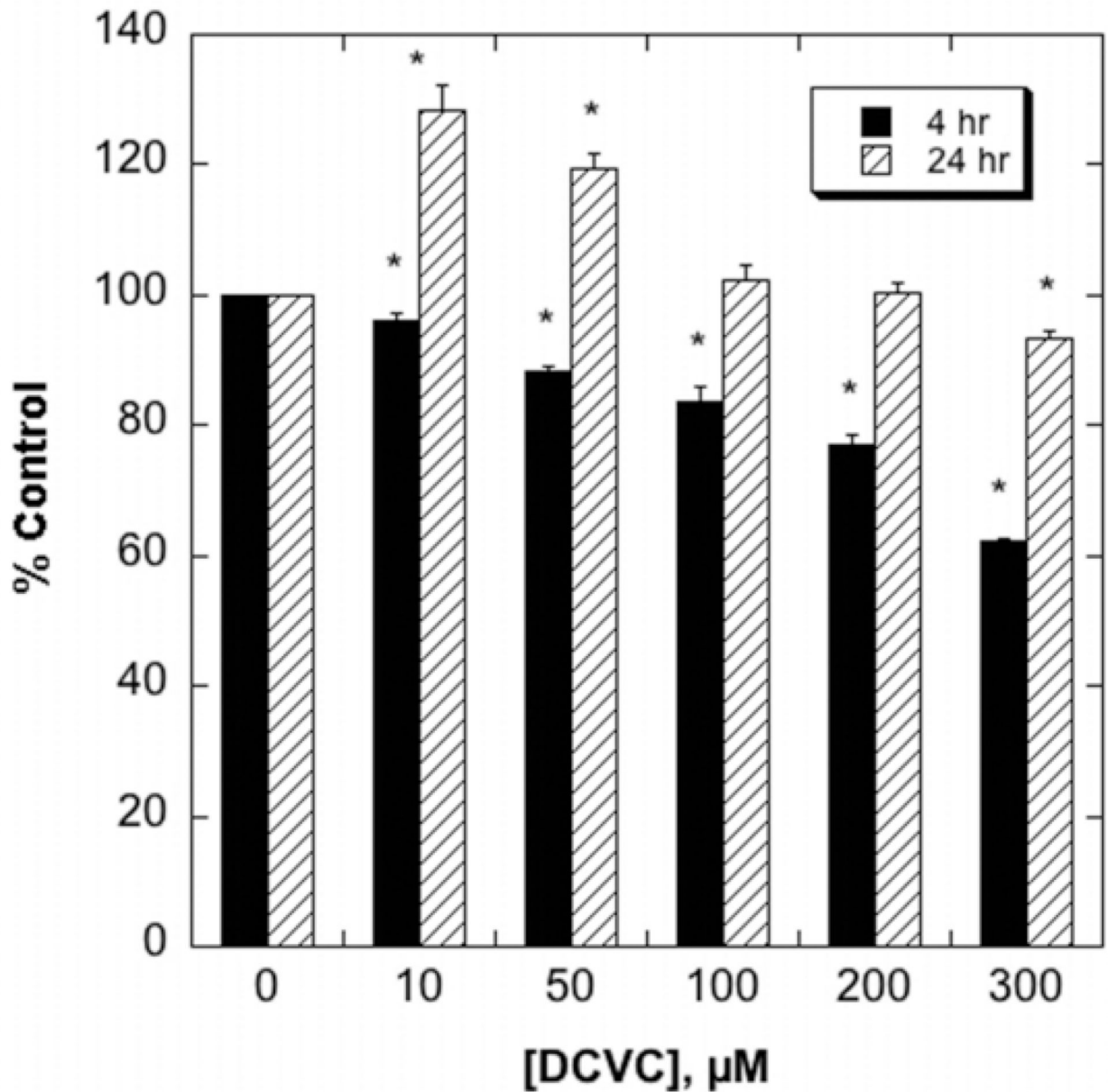


Figure 2.

Figure 2. DCVC-induced proliferation assessed by MTT reduction

Confluent primary cultures of hPT cells grown in collagen-coated, 24-well plates were incubated for 4 or 24 hr with the indicated concentrations of DCVC. MTT reduction was measured spectrophotometrically and is expressed as percent control. Data are means \pm SEM of measurements from 4 separate cell cultures, each deriving from a different kidney.

*Significantly different ($P < 0.05$) from the corresponding control cells.

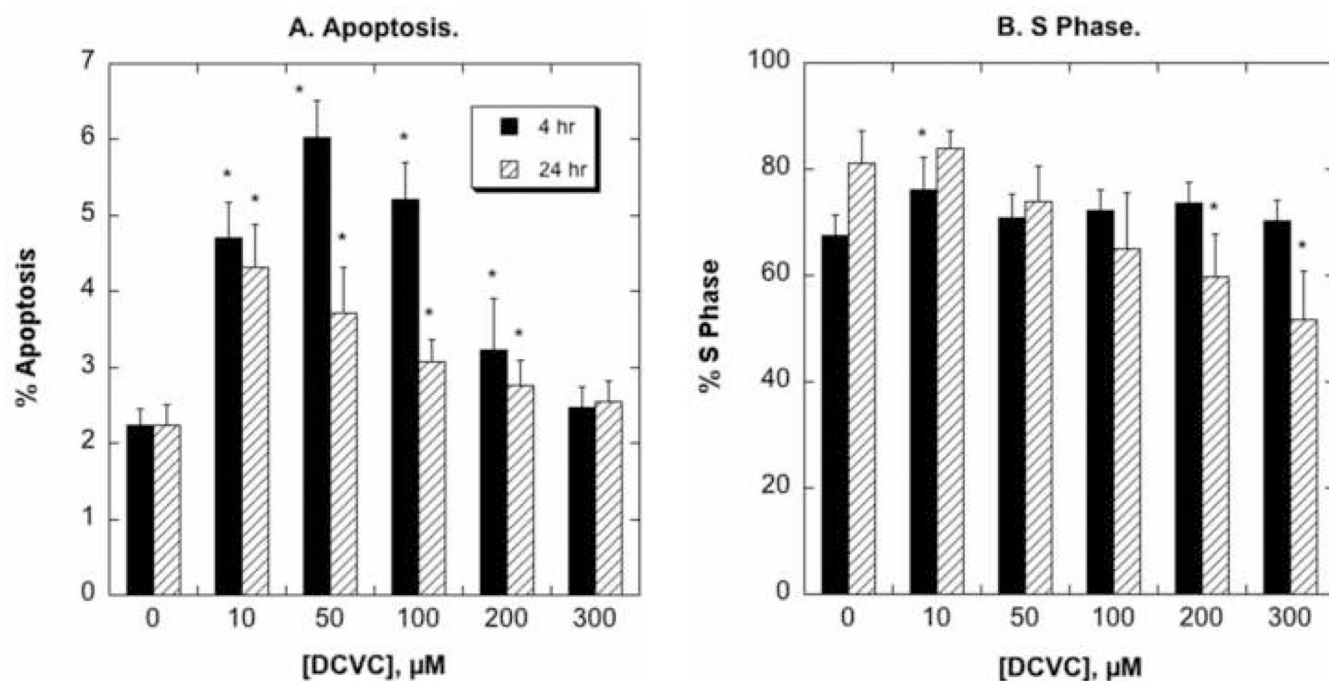


Figure 3.

Figure 3. DCVC-induced apoptosis and cell proliferation assessed by flow cytometry and FACS analysis

hPT cells grown in collagen-coated, 6-well plates were incubated for 4 or 24 hr with the indicated concentrations of DCVC. Cells were stained with propidium iodide and cell cycle status was analyzed by flow cytometry and FACS analysis. Results are the percentage of cells undergoing apoptosis (sub-diploid) (A) and the percentage of cell in S-phase. Values are means \pm SEM of measurements from 4 separate cell cultures, each deriving from a different kidney. *Significantly different ($P < 0.05$) from the corresponding control cells.

A. Control.

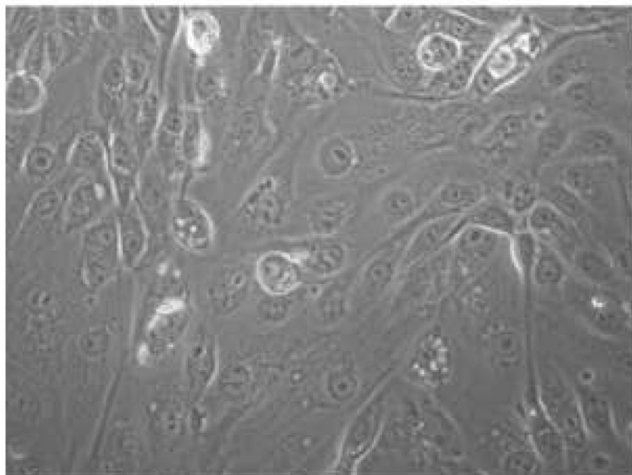
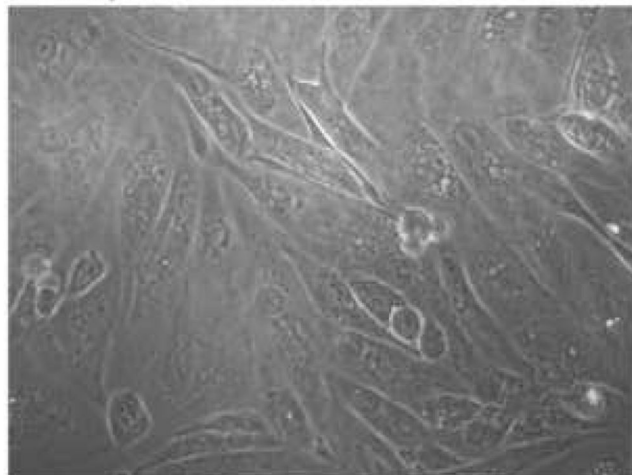
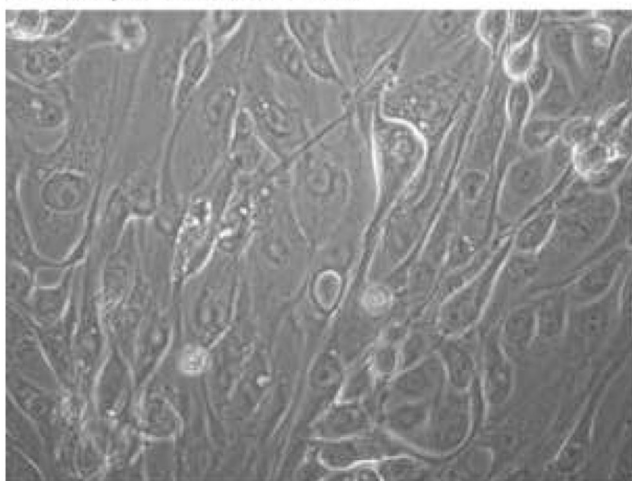
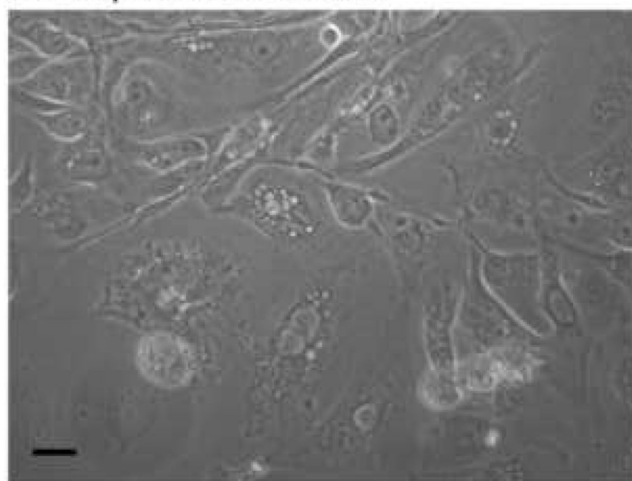
B. 50 μ M DCVC-4hr.C. 50 μ M DCVC-8 hr.D. 50 μ M DCVC-24 hr.

Figure 4.

Figure 4. Time-dependent changes in morphology induced by DCVC

hPT cells were cultured for 5 days in supplemented, serum-free, hormonally-defined DMEM:F12 medium on collagen-coated, 35-mm polystyrene dishes until they were confluent. Cells were then incubated for the indicated times up to 24 hr with either medium (= Control) or 50 μ M DCVC. At the indicated times, photomicrographs were taken at 196X magnification on a Carl-Zeiss Confocal Laser Microscope. Bar = 5 μ m.

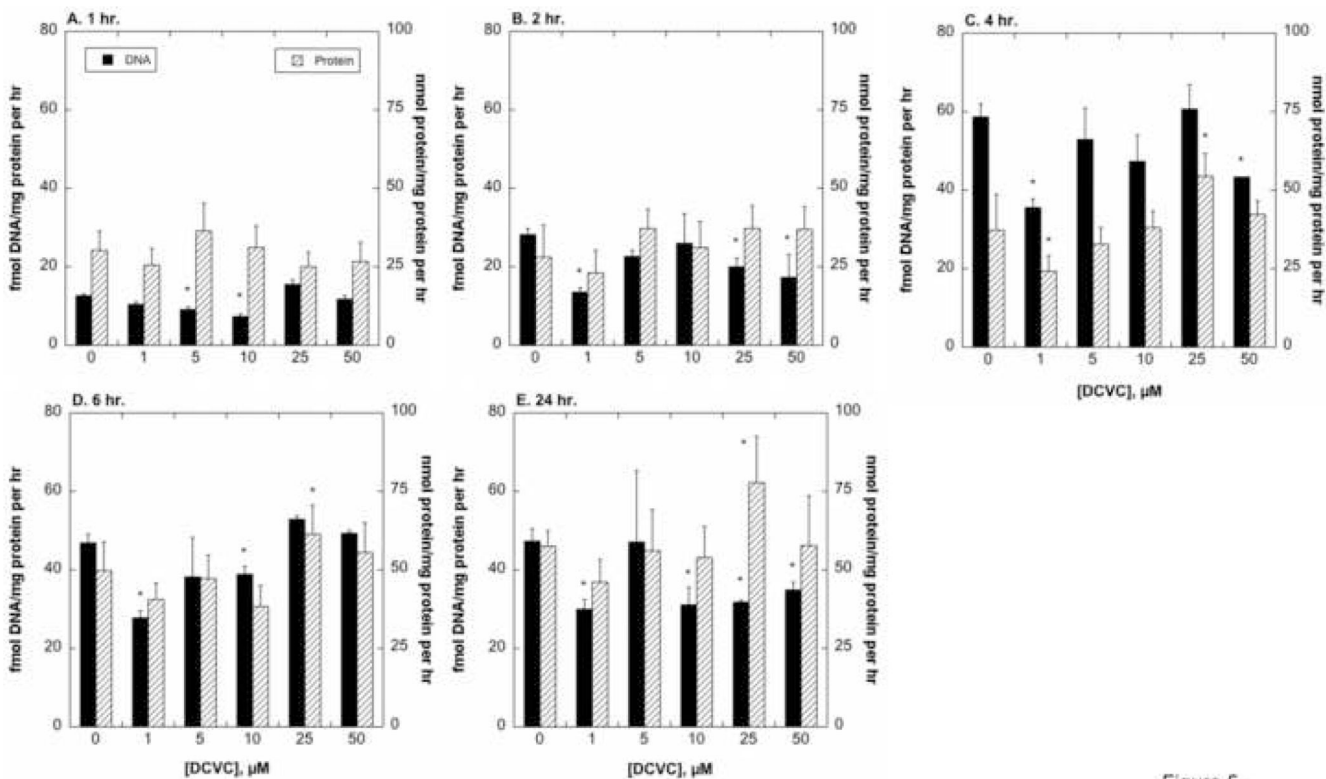


Figure 5.

Figure 5. DCVC-induced changes in DNA and protein synthesis

Confluent hPT cells grown on collagen-coated, 24-well plates were incubated with the indicated concentrations of DCVC for up to 24 hr. At the specified times, dishes were washed and then incubated for 1 hr with precursors for DNA, including [methyl-³H]-dTTP, for measurement of rates of DNA synthesis (A), or with [4,5-³H]-L-leucine for measurement of rates of protein synthesis (B). Samples were processed for determination of radioactivity in the acid-insoluble fraction and results were normalized to protein content. Results are the means ± SEM of measurements from 4 separate cell cultures, each deriving from a different kidney. *Significantly different (*P* < 0.05) from corresponding control values.

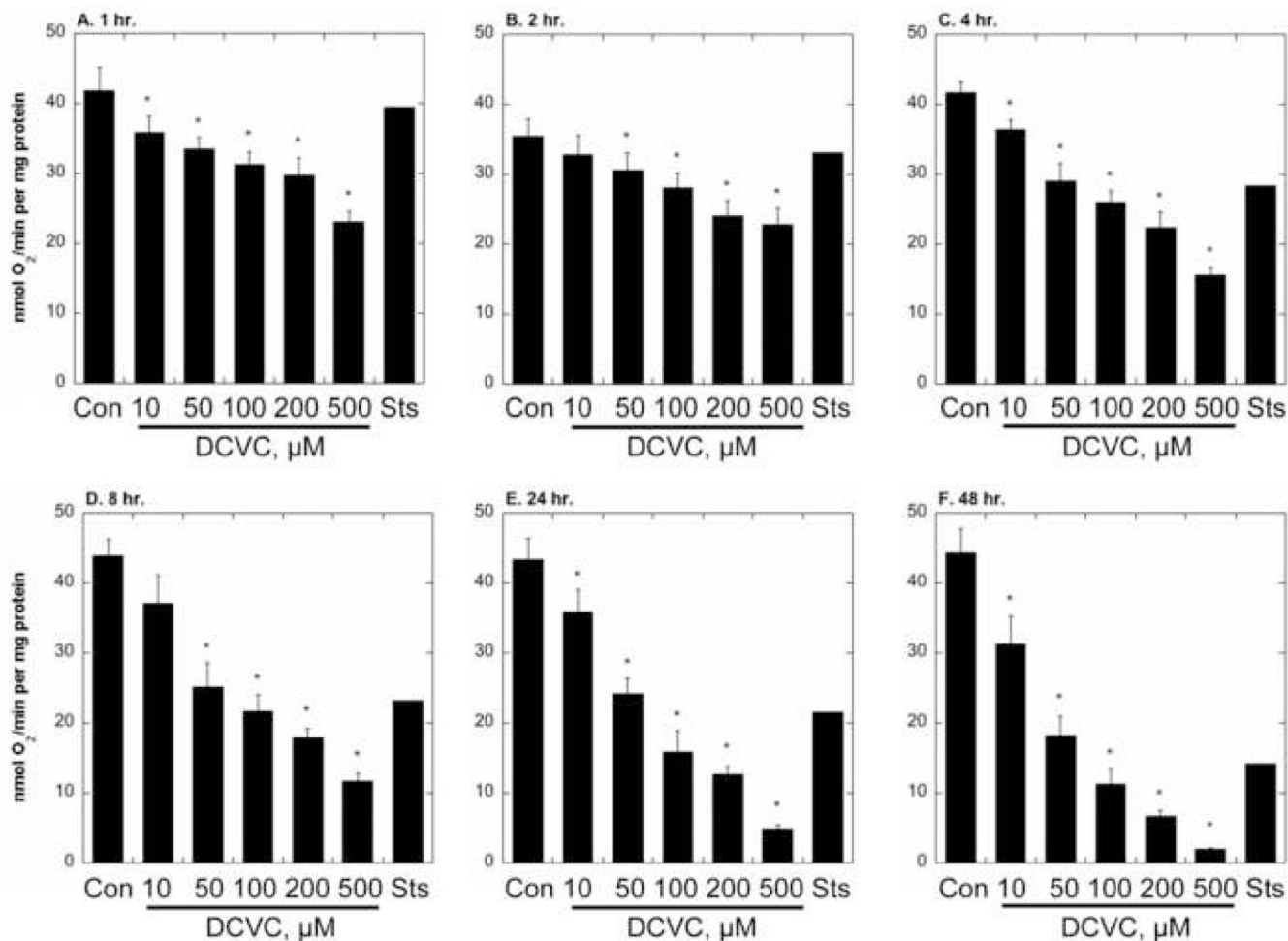


Figure 6.

Figure 6. Time- and concentration-dependent inhibition of cellular respiration by DCVC
 Confluent hPT cells grown on collagen-coated, T-25 flasks were incubated up to 48 hr with PBS (= Control, Con), the indicated concentrations of DCVC, or 1 μM staurosporine (Sts). At the indicated times, cells were released from flasks by brief treatment with trypsin/EDTA, resuspended in PBS at a cell concentration of 2×10^6 /ml, and were added to the Oxygraph electrode chamber for measurement of succinate-stimulated O₂ consumption. Results are means ± SEM of measurements from 4 separate cell cultures, each deriving from a different kidney, except for incubation with Sts, which were averages of measurements from 2 separate cell cultures. *Significantly different ($P < 0.05$) from corresponding control values.

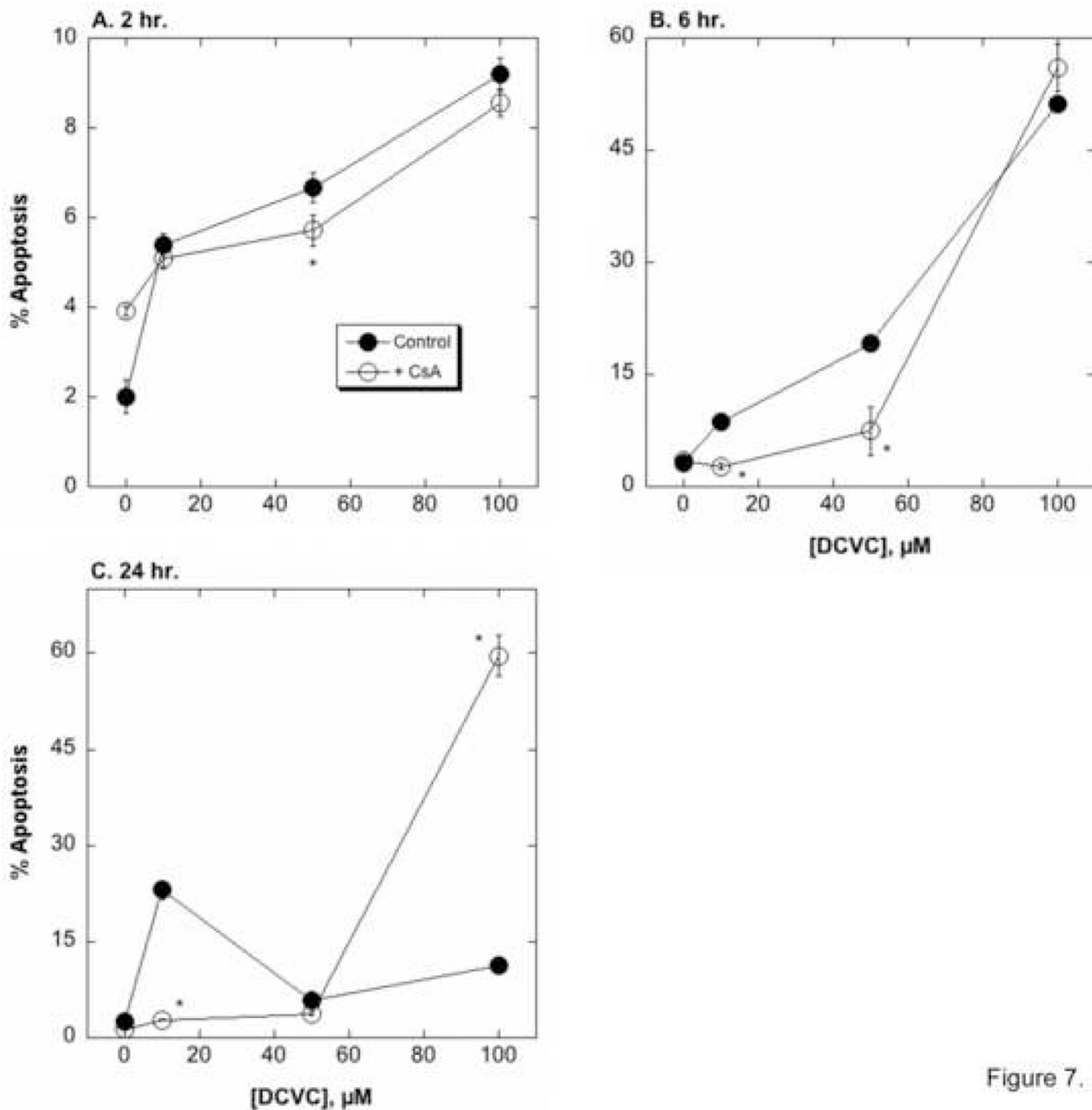


Figure 7.

Figure 7. Effect of CsA on DCVC-induced apoptosis

hPT cells grown in collagen-coated, 6-well plates were incubated for 4 or 24 hr with the indicated concentrations of DCVC in the absence or presence of 0.5 nmol CsA/mg protein. Cells were stained with propidium iodide and cell cycle status was analyzed by flow cytometry and FACS analysis. Results are the percentage of cells undergoing apoptosis (sub-diploid) and are means \pm SEM of measurements from 4 separate cell cultures, each deriving from a different kidney. Where not visible, error bars were within the bounds of the data point. *Significantly different ($P < 0.05$) from the corresponding control cells.

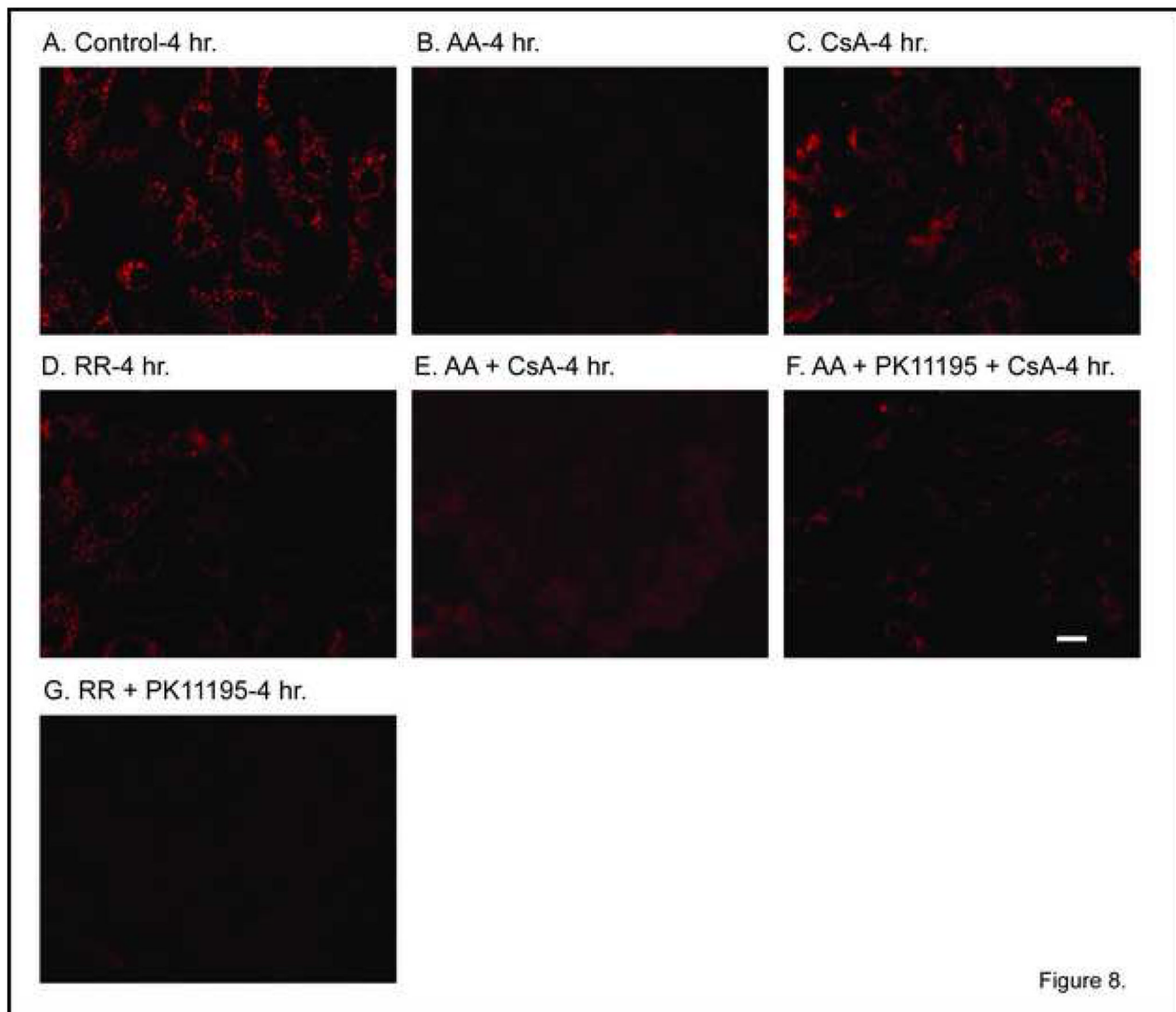


Figure 8.

Figure 8. Effect of mitochondrial inhibitors on mitochondrial membrane potential

Confluent, primary cultures of hPT cells were grown on collagen-coated, glass cover slips in 35-mm tissue culture dishes and were incubated for 4 hr with media (= Control) or mitochondrial inhibitors, added singly or together, as indicated, at the following concentrations: 1 μ M AA, 0.5 nmol CsA/mg protein, 30 μ M RR, and 120 μ M PK11195. JC-1 fluorescence was measured by confocal microscopy assessing the emission of punctate red (\sim 590 nm) in polarized mitochondria using 488-nm excitation. Red fluorescence is shown. Polarized mitochondria are indicated by yellow-red punctate staining whereas depolarized mitochondria exhibit diffuse or no staining. White bars = 5 μ m.

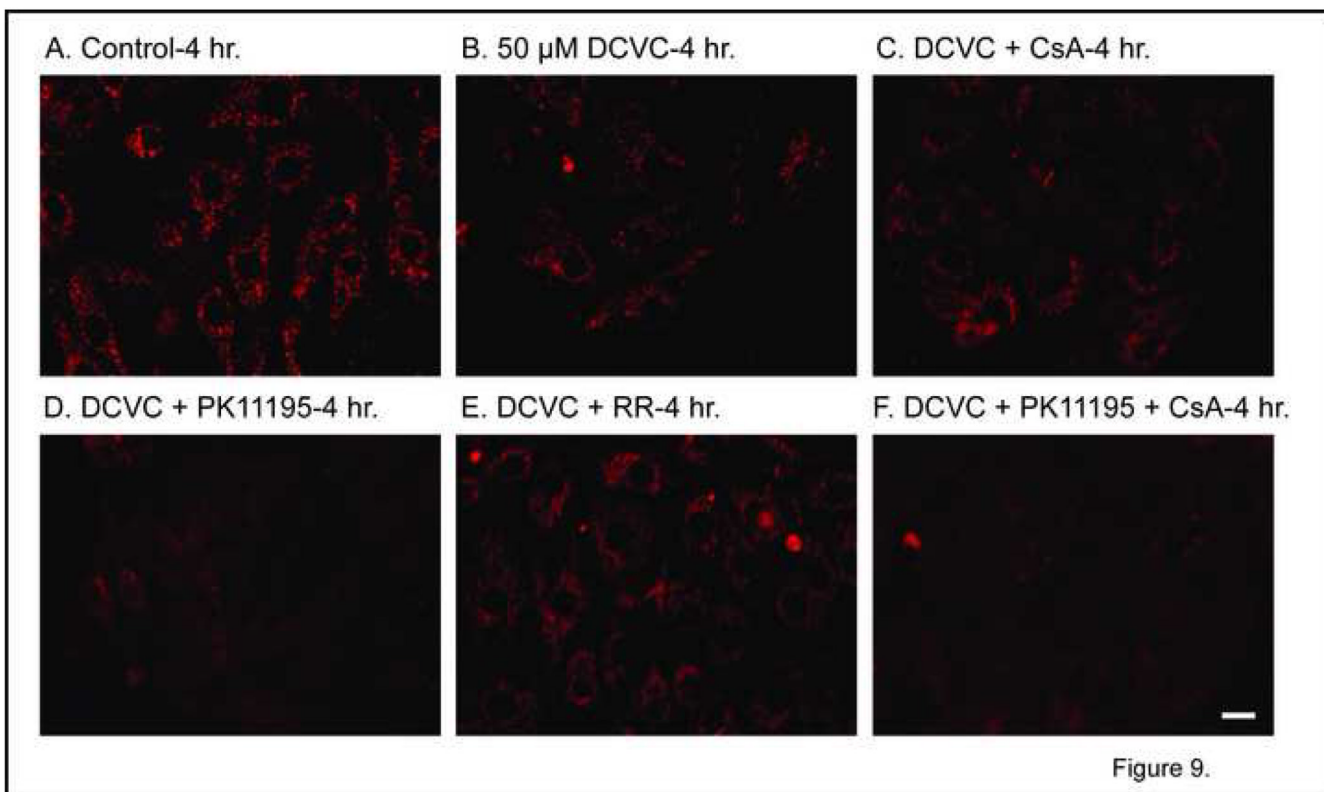
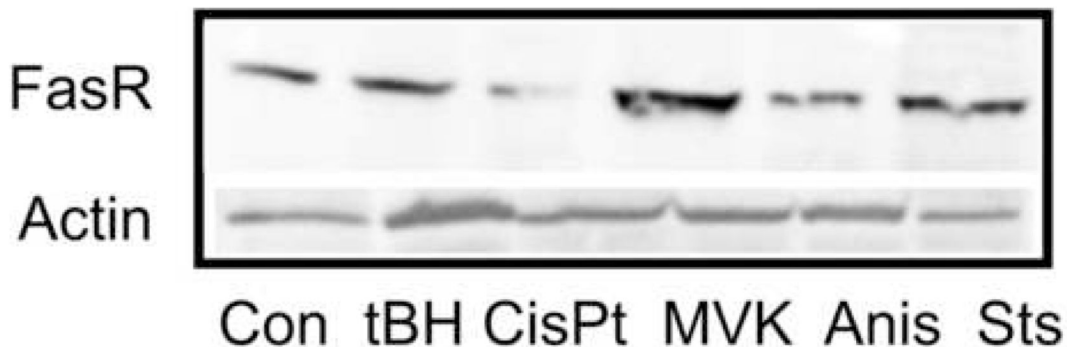


Figure 9. Effect of DCVC and mitochondrial inhibitors on mitochondrial membrane potential
Confluent, primary cultures of hPT cells were grown on collagen-coated, glass cover slips in 35-mm tissue culture dishes and were incubated for 4 hr with media (= Control) or 50 μ M DCVC alone or with the indicated mitochondrial inhibitors as in Fig. 8. JC-1 fluorescence was measured by confocal microscopy as described in the legend to Fig. 8. White bars = 5 μ m.

A. Model toxicants.



B. DCVC and TRI.

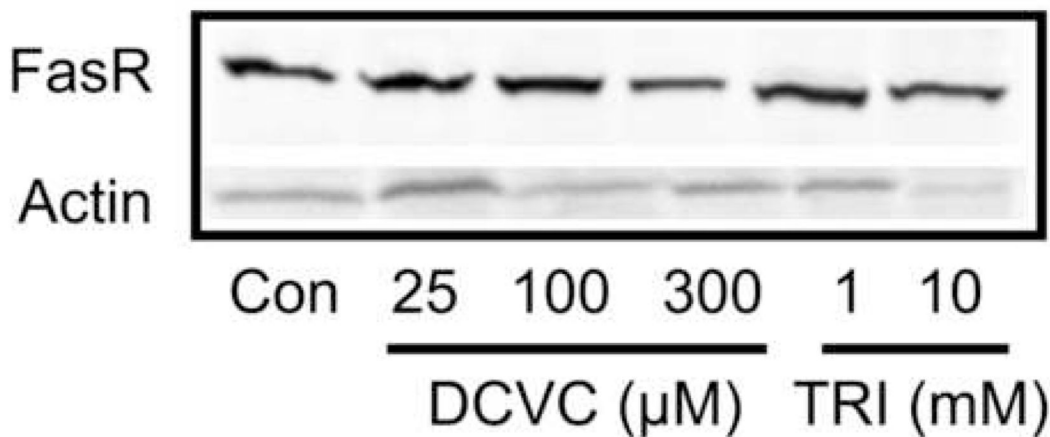


Figure 10.

Figure 10. Effects of DCVC and LPS on FasR expression

Primary cultures of hPT cells were grown on collagen-coated T-75 flasks to ~90-100% confluence and were treated for 4 hr with either (A) media (= Control [Con]) or model chemicals, including 50 μ M tBH, 100 μ M CisPt, 100 μ M MVK, 10 μ g/ml anisomycin (Anis), or 1 μ M Sts, or (B) media (= Control [Con]), DCVC (25, 100, or 300 μ M), or TRI (1 or 10 mM). Western blot analysis was conducted using a rabbit polyclonal antibody to the FasR protein (MW = 48 kDa) that recognizes the human FasR protein. Parallel samples were also run using a polyclonal antibody that detects human actin.

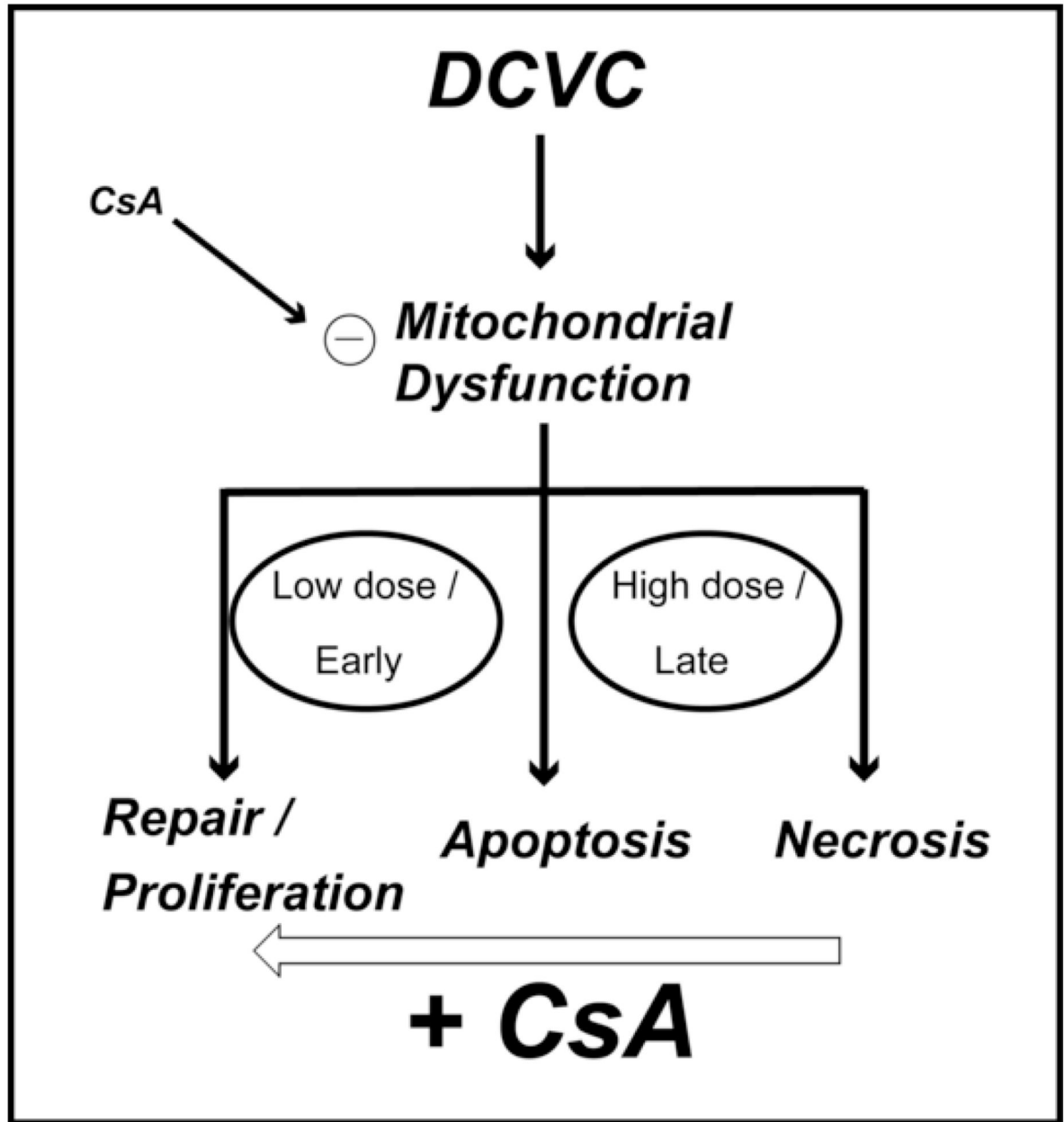


Figure 11.

Figure 11. Simplified scheme illustrating the influence of CsA on DCVC-induced mitochondrial dysfunction and cytotoxicity in hPT cells.

Table 1

Effect of DCVC and mitochondrial inhibitors on ATP concentrations of hPT cells

Incubation	ATP (% Control)
Control	100 ± 5.1
1 mM KCN + 0.1 mM Iodoacetate (KCN/IAA) [0.5 hr]	22.6 ± 7.3
1 μM Antimycin A (AA)	78.7 ± 3.3
1 μM Staurosporine (Sts)	78.7 ± 8.4
50 μM <i>tert</i> -Butyl hydroperoxide (tBH)	18.2 ± 2.1
DCVC:	
10 μM	80.0 ± 2.1
50 μM	71.7 ± 3.9
100 μM	60.7 ± 13.4
200 μM	61.0 ± 8.0
300 μM	48.3 ± 8.4

Primary cultures of hPT cells were grown to ~80% confluence and then incubated with the indicated additions for 24 hr, except for KCN/IAA as noted. Cellular contents of ATP were determined by a luminescence assay and are expressed as the percent of control. Control = 8.63 nmol ATP/mg protein. Results are means ± SEM of measurements from 3 separate cell cultures, each derived from a different kidney. All values were significant different ($P < 0.05$) from those for Control cells.

Table 2

Effect of DCVC and mitochondrial inhibitors on caspase activities of hPT cells

Incubation	Caspase-3/7		Caspase-8	
	4 hr	24 hr	4 hr	24 hr
Control	100 ± 6.4	100 ± 4.1	100 ± 5.5	100 ± 4.2
1 μM Antimycin A (AA)	90.5 ± 6.5	115 ± 10	74.6 ± 4.1*	155 ± 7*
1 μM Staurosporine (Sts)	212 ± 11*	262 ± 15*	175 ± 8*	137 ± 6*
DCVC:				
10 μM	115 ± 5*	92.5 ± 4.3	117 ± 6*	108 ± 4
50 μM	141 ± 8*	94.1 ± 5.5	107 ± 6	110 ± 4*
100 μM	105 ± 6	82.3 ± 4.4*	94.2 ± 4.1	124 ± 10*
200 μM	85.5 ± 3.5*	67.7 ± 4.1*	82.2 ± 4.5*	97.6 ± 4.4
300 μM	74.7 ± 3.5*	52.1 ± 3.2*	72.5 ± 2.7*	86.4 ± 4.2*

Primary cultures of hPT cells were grown to ~80% confluence and then incubated with the indicated additions for 4 hr or 24 hr. At the end of the incubation time, cells were washed, scraped into 100 μl of PBS in 96-well plates, and then 100 μl of either the Caspase-Glo 3/7 or 8 reagent was added. After 2 hr incubation in the dark, plates were read in luminescence mode in a SpectraMax 2 plate reader (Molecular Devices). Results are expressed as relative luminescence normalized to protein relative to controls (set at 100 for each experiment) and are means ± SEM of measurements from 3 separate cell cultures, each derived from a different kidney.

* Significantly different ($P < 0.05$) from the corresponding control value.